

Synthesis of chalcone-containing zinc and cobalt metallophthalocyanines; investigation of their photochemical, DPPH radical scavenging and metal chelating characters

Arif Baran^{1*}, Emel Karakılıç¹, Özlem Faiz² and Furkan Özen¹

¹Department of Chemistry, Faculty of Arts and Sciences, Sakarya University, 54187, Sakarya, Türkiye

²Department of Chemistry, Faculty of Arts and Sciences, ²RTE University 53100, Rize, Türkiye

(Received May 02, 2020; Revised June 16, 2020; Accepted June 20, 2020)

Abstract: In this study, two new phthalocyanines (M = Zn and Co) were synthesized using the (*E*)-4-(4-(3-(4-(benzyloxy)phenyl)acryloyl)phenoxy)phthalonitrile (**3**) as ligand prepared from the chemical reaction of 4-nitrophthalonitrile with (*E*)-3-(4-(benzyloxy)phenyl)-1-(4-hydroxyphenyl)prop-2-en-1-one (**2**). All compounds were characterized using by ¹H-NMR, ¹³C-NMR, UV-Vis, FT-IR, and MALDI-TOF mass spectra. Singlet oxygen quantum yields of the synthesized compounds, aggregates in different solutions, metal chelating and 2,2-Diphenyl-1-picrylhydrazyl (DPPH) radical scavenging properties were reported.

Keywords: Phthalocyanines; photochemical studies; singlet oxygen; quantum yields; metal chelating; DPPH radical scavenging. ©2020 ACG Publication. All right reserved.

1. Introduction

Phthalocyanines (Pcs) and Metallophthalocyanines (MPcs) have been studied for a wide range of applications in view of their distinct and unique optical, spectroscopic, electronic, electrochemical, and thermal properties.¹⁻³ The presence of diamagnetic metals in phthalocyanines (such as zinc, aluminum, silicon) makes them a useful photosensitizers in photodynamic therapy (PDT) with their high quantum yields and long triplet lifetime.⁴⁻⁷ PDT requires the use of photosensitive molecules known as photosensitizers. Photoactivation causes the formation of singlet oxygen, which produces peroxidative reactions that can cause cell damage and death.⁸ In the earlier studies, hematoporphyrin derivatives and porfimer sodium (photofrin) were successfully used in PDT and, many second-generation photosensitizer, porphyrines and derivatives, have been synthesized for this purpose.^{9,10}

The ligands prepared via Claisen-Schmidt condensation are known as chalcones which are belonging to the flavonoid family.¹¹⁻¹² Chalcones are aromatic pigments with antioxidant effect on fruits, vegetables and various wounded plant tissues, which act as chemical messenger, physiological regulator and inhibitors of cell cycle. The role of flavonoids against cancer, aging, atherosclerosis, ischemic injury, inflammation and neurodegenerative diseases (Parkinson, Alzheimer) have been reported¹³⁻¹⁴. Their antioxidant, anti-tumor, anti-inflammatory and antiviral activities were seriously discussed in the literature.¹³⁻¹⁹ In addition, dissolution force of chalcone-based ligands in organic solvents increased the interest in chalcone-fused phthalocyanines.

* Corresponding author: E-mail: abaran@sakarya.edu.tr

The article was published by ACG Publications

<http://www.acgpubs.org/journal/organic-communications> © April-June 2020 EISSN:1307-6175

DOI: <http://doi.org/10.25135/acg.oc.80.20.05.1639>

Regarding to those properties, synthesis of chalcone-containing zinc and cobalt metallophthalocyanines and their photochemical properties, DPPH radical scavenging and metal chelating capacities were reported herein.

2. Experimental

2.1. General

Benzyl chloride (Sigma-Aldrich, reagent plus(R), 99%), 4-hydroxybenzaldehyde (Sigma-Aldrich, 98%), 4-hydroxyacetophenone (Sigma-Aldrich, 99%), 4-nitrophthalonitrile (Sigma-Aldrich, 99%), thionyl chloride (SOCl₂) (Sigma-Aldrich, reagent plus(R), ≥99%), potassium carbonate (K₂CO₃) (Alfa Aesar, anhydrous, 99%), 1,8-diazabicyclo[5.4.0]undec-7-ene (DBU) (Merck, 98%), zinc acetate dihydrate Zn(OAc)₂·2H₂O (Sigma-Aldrich, reagent grade), cobalt (II) acetate tetrahydrate Co(OAc)₂·4H₂O (Sigma-Aldrich, reagent grade), sodium sulfate (Na₂SO₄) (Alfa Aesar, ACS, 99.0% min), 2,2',2'',2'''-(ethane-1,2-diylidinitrilo)tetraacetic acid (EDTA) (Sigma-Aldrich, ≥98.0% (KT)), ferrous chloride (FeCl₂) (Sigma-Aldrich, reagent plus (R), 98%) were used as supplied without further purification. Reactions under anhydrous conditions were performed in dried solvents (such as, N,N-dimethylformamide (DMF), dichloromethane (DCM), dimethyl sulfoxide (DMSO), tetrahydrofuran (THF) and ethanol (EtOH)) under argon atmosphere. Silica gel 60 (40–63 μm, Fluka) was used for chromatography. ¹H NMR and ¹³C NMR spectra were recorded in CDCl₃ on a VARIAN Infinity Plus 300 MHz NMR spectrometer. Chemical shifts were expressed in ppm relative to CDCl₃ (δ 7.26 and 77.0 for ¹H and ¹³C NMR, respectively) and Tetramethylsilane (TMS) was as a internal standard. IR spectra were recorded on an Ati Unicam Mattson 1000 Series FT-IR (ATR system) spectrometer. MALDI-TOF spectra were taken on Bruker Daltonics flex Analysis. Electronic absorption spectra were measured on a Shimadzu UV 2600 UV-Vis spectrophotometer

2.2. Chemistry

2.2.1 Synthesis of 4-(benzyloxy)benzaldehyde (1)

4-Hydroxy benzaldehyde (1.0 g, 8.19 mmol) in DMF was added K₂CO₃ (1.130 g, 8.19 mmol). The mixture was stirred at room temperature for 30 min. Benzyl chloride (1.400 g, 8.19 mmol) was added dropwise, and the mixture was stirred for 3 h, and the reaction mixture was poured dropwise into ice water (250 mL) and stirred. The white solid product was filtered and washed with water, dried and recrystallized in ethanol to afford **1**. Yield: 1.51 g (87%), m. p.: 69-71 °C. IR $\nu_{\max}/\text{cm}^{-1}$: 3362 cm⁻¹ (Ar-H); 2829 cm⁻¹ (aliphatic C-H); 1685 cm⁻¹ (C=O); 1598, 1572, 1508 cm⁻¹ (Ar-C=C); 1018 cm⁻¹ (C-O-C). ¹H NMR (300 MHz, CDCl₃) δ ppm: 9.86 (s, 1H, CHO), 7.82 (quasi d, H₂ and H₆, 2H, *J* = 9.0Hz), 7.15 (quasi d, H₃ and H₅, 2H, *J* = 9.0Hz), 7.48 – 7.32 (m, 5H, Ph), 5.12 (s, 2H, PhCH₂O). ¹³C NMR (75 MHz, CDCl₃) δ ppm: 190.77, 163.62, 135.85, 131.93, 129.96, 128.65, 128.26, 127.44, 115.04, 70.13.

2.2.2 Synthesis of (E)-3-(4-(benzyloxy)phenyl)-1-(4-hydroxyphenyl)prop-2-en-1-one (2)

Compound **2** was prepared according to the method reported in the literature.²⁰ 4-(Benzyloxy)benzaldehyde (0.500 g, 2.36 mmol) and 4-hydroxyacetophenone (0.321 g, 2.36 mmol) were mixed in ethanol, and then thionyl chloride (0.5 mL) was added. After stirring for 14 h, the mixture was added to water. The product was filtered and washed with cold ethanol to afford compound **2** as yellow crystal. Yield: 0.69 g (89%), m. p.: 187-189 °C. IR $\nu_{\max}/\text{cm}^{-1}$: 3059 cm⁻¹ (OH); 3049 cm⁻¹ (Ar-H); 2849 cm⁻¹ (aliphatic C-H); 1641 cm⁻¹ (C=O); 1597, 1586 cm⁻¹ (Ar-C=C); 1037 (C-O-C). ¹H NMR (300 MHz, CDCl₃ / CD₃OD: 5/1) δ ppm: 7.97 (quasi d, 2H, H₂' and H₆', *J* = 9.0 Hz), 7.76 (d, CH=CH-CHO, 1H, *J*=15 Hz), 7.62 (quasi d, 2H, H₂" and H₆" *J* = 9.0 Hz), 7.10 (d, 2H, H₃' and H₅', *J* = 9.0 Hz), 6.92 (d, 2H, H₃" and H₅" *J* = 9.0 Hz), 5.12 (s, 2H, PhCH₂O). ¹³C NMR (75

MHz, CDCl₃ / CD₃OD: 5/1) δ ppm: 189.48, 161.57, 160.68, 143.96, 136.38, 131.10, 130.20, 128.69, 128.20, 127.96, 127.54, 119.63, 115.44(2C), 115.24, 70.11.

2.2.3 Synthesis of (*E*)-4-(4-(3-(4-(benzyloxy)phenyl)acryloyl)phenoxy)phthalonitrile (**3**)

A mixture of 4-nitrophthalonitrile (0.6 g, 3.45 mmol) and (*E*)-3-(4-(benzyloxy)phenyl)-1-(4-hydroxyphenyl)prop-2-en-1-one (**2**) (1.14 g, 3.45 mmol) in 25 mL of dry DMF was stirred at 50 °C under N₂. Anhydrous K₂CO₃ (0.57 g, 4.14 mmol) was added to the mixture for over a period of 1.5 h. After stirring the reaction mixture for a further 24 h, the undissolved salt was removed by filtration. The reaction mixture was added dropwise into ice water (250 mL). The organic phase was extracted with DCM (250 mL) and dried on Na₂SO₄. After evaporation of the solution under reduced pressure gave yellow residue. The residue was purified by silica gel column chromatography to afford **3**. Yield: 1.20 g (76%), m. p.: 198 °C. IR $\nu_{\max}/\text{cm}^{-1}$: 3073 cm⁻¹ (Ar-H); 2949 cm⁻¹ (aliphatic C-H); 2230 cm⁻¹ (C≡N); 1655 cm⁻¹ (C=O); 1588, 1575, 1508 cm⁻¹ (C=C); 1025 cm⁻¹ (C-O-C). ¹H NMR (300 MHz, CDCl₃) δ ppm: 8.19 (quasi d, 2H, H_{3'} and H_{5'}, $J = 9.0\text{Hz}$), 7.84 (d, 1H, H_{3''}, $J = 15\text{Hz}$), 7.78 (overlapped 2 H), 7.51 – 7.23 (m, 9 ArH), 7.20 (d, 2H, H_{2''} and H_{6''}, $J = 9.0\text{Hz}$), 7.03 (d, 2H, H_{3''} and H_{5''}, $J = 9.0\text{Hz}$), 5.13 (s, 2H, PhOCH₂). ¹³C NMR (75 MHz, CDCl₃) δ ppm: 188.97, 161.29, 160.86, 157.35, 145.58, 136.50, 135.85, 131.46, 130.67, 128.95, 128.48, 127.77, 122.59, 122.41, 120.38, 119.26, 118.11, 115.58, 115.06, 110.06, 70.36.

2.2.4 General Procedure for Preparation of the Synthesis of zinc (II) phthalocyanine (**4a**)

A mixture of **3** (0.1 g, 0.22 mmol), Zn(OAc)₂·2H₂O (0.058 g, 0.26 mmol) and 2-3 drops 1,8-diazabicyclo[5.4.0]undec-7-en (DBU) were stirred at 130 °C in dry DMF under N₂ for 24 h. The reaction mixture was cooled to rt and undissolved salt was removed by filtration. The dark green solution was poured into ice-water (100 mL) and stirred for 1 h and filtered. The filtrates were washed with a plenty of water then hot ethanol and removed of the unreacted organic materials. The product was dried in the oven to give a crude **4a** which is soluble DCM, THF, DMF and DMSO. Then the it was purified using column chromatography on silica gel. The chromatography was repeated and various solution ratios (DCM / THF, DCM / EtOH, THF / EtOH) were used. All purified fractions were collected to give compound **4a** as green solid. Yield: 0.05 g (43%), m. p.: >350 °C. IR $\nu_{\max}/\text{cm}^{-1}$: 3063 cm⁻¹ (Ar-H); 2958 cm⁻¹ (aliphatic C-H); 1657 cm⁻¹ (C=O); 1594, 1574, 1505 cm⁻¹ (C=N, C=C); 1025 cm⁻¹ (C-O-C). UV-Vis (DMF), λ_{\max} , nm: 679.5, 618, 354.5. MALDI-TOF MS: m/z [M]⁺ calcd. for C₁₂₀H₈₀N₈O₁₂Zn: 1891.38; found [M + H]⁺ 1891.17. Elemental analysis for [C₁₂₀H₈₀N₈O₁₂Zn]: C, 76.20; H, 4.26; N, 5.92. Found: C, 76.28; H, 4.32; N, 5.99%.

2.2.5 General Procedure for Preparation of the Synthesis of Cobalt (II) phthalocyanine (**4b**)

A mixture of **3** (0.1 g, 0.22 mmol), Co(OAc)₂·4H₂O (0.065 g, 0.26 mmol) and 2-3 drops 1,8-diazabicyclo[5.4.0]undec-7-en (DBU) were stirred at 130 °C of dry DMF under N₂ for 24 h. The reaction mixture was cooled down to room temperature. The undissolved salt was removed by filtration. After the dark green product was poured into ice-water (100 mL) and stirred. It was filtered and washed with water, hot ethanol, remove the unreacted organic materials. The resulting dark green product was dried in an oven. This compound is readily soluble DCM, THF, DMF and DMSO. Then the dark green residue was purified using column chromatography on silica gel. The chromatography were repeated with various solution ratios (DCM / THF, DCM / EtOH, THF / EtOH). All purified fractions were collected to afford **4b** as green solid. Yield: 0.06 g (53%), m. p.: >350 °C. IR $\nu_{\max}/\text{cm}^{-1}$: 3066 cm⁻¹ (Ar-H); 2930 cm⁻¹ (aliphatic C-H); 1656 cm⁻¹ (C=O); 1592, 1556, 1507 cm⁻¹ (C=N, C=C); 1025 cm⁻¹ (C-O-C). UV-Vis (DMF), λ_{\max} , nm: 667.5, 602.5, 345.5. MALDI-TOF MS: m/z [M]⁺ calcd. for C₁₂₀H₈₀N₈O₁₂Co: 1884.94; found [M + H]⁺ 1884.78. Elemental analysis for [C₁₂₀H₈₀N₈O₁₂Co]: C, 76.47; H, 4.28; N, 5.94. Found: C, 76.55; H, 4.25; N, 5.92%.

2.3. Metal Ions Chelating Effects Assay

Metal chelating activities of the phthalocyanines were examined using ferrous ion–ferrozine complex method. Results were compared to EDTA, which was used as a reference compound. 500 μL of varying concentrations (25–100 μM) of phthalocyanine was prepared and added to 2 mM, 50 μL FeCl_2 and 5 mM, 100 μL ferrozine. After 10 minute incubation at room temperature, optical density of the samples was measured at 562 nm. A control assay mixture without phthalocyanine was also studied. All experiments were repeated three times and the results were stated as the mean \pm standard deviation (S.D.). Metal chelating effect was calculated using the equation below.²¹⁻²⁸

$$\text{Metal chelating effect (\%)}: \left[\frac{A_{\text{control}} - A_{\text{sample}}}{A_{\text{control}}} \right] \times 100 \quad (\text{Eq. 1})$$

The reduction of DPPH induces the radical to change color (violet to yellow) and this change is quantifiable at 517 nm.

2.4. DPPH Radical Scavenging Activity Assay

DPPH radical scavenging activities of Pcs were measured to predict their in vitro antioxidant activities.²⁹⁻³⁰ Briefly, 0.5 mL of Pcs **4a** and **4b** at different concentrations in DMSO were added to a freshly prepared 1 mL of 0.1 mM DPPH in methanol. The assay mixtures were incubated in dark for 50 minutes, at room temperature. Their optical density of the assay mixtures was measured at 517 nm. A control without Pcs and a gallic acid standard was studied at the same conditions. All experiments were repeated three times and the results were stated as the mean \pm standard deviation (S.D.). Free radical scavenging effect of Pcs was calculated using the equation (3).

2.5. Singlet Oxygen Measurements

The compound with singlet oxygen quencher was irradiated in the Q band region using photo-irradiation apparatus.³¹ Quantum yields Φ_{Δ} for singlet oxygen were performed according to relative method ZnPc in DMSO. DPBF (1,3-diphenylisobenzofuran) was used as a chemical quencher. The experimental part was performed in DMSO. To a solution of **4a** was added a singlet oxygen quencher (3×10^{-5} mol/dm³) and the intensity of light was applied as 8.15×10^{15} photon s⁻¹ cm⁻² Eq. (2).³²

$$\Phi_{\Delta} = \Phi_{\Delta}^{\text{Std}} \frac{R \cdot I_{\text{abs}}^{\text{Std}}}{R^{\text{Std}} \cdot I_{\text{abs}}} \quad (2)$$

Where,

$\Phi_{\Delta}^{\text{Std}}$ defines the singlet oxygen quantum yield (Φ_{Δ}) for the standard Zn-Pc ($\Phi_{\Delta}^{\text{Std}} = 0.67$ in DMSO).

R and R^{Std} are DPBF photo-bleaching properties in the presence of **4a**.

I_{abs} and $I_{\text{abs}}^{\text{Std}}$ are the rate of light used for samples and standard.^{33,34}

2.6. Photodegradation Measurements

Photodegradation quantum yield (Φ_{Δ}) was measured by using Eq. (3), to examine the changes in fluorescence in the course of degradation of the compound exposed to light. During the photodegradation of phthalocyanine compounds, the decrease in Q band was determined and the trends of the calibration graphs were calculated in specific time intervals.³⁵⁻³⁶ Photodegradation quantum yield (Φ_{Δ}) determination was described in the literature.²⁴

$$\Phi_d = \frac{(C_0 - C_t) \cdot V \cdot N_A}{I_{abs} \cdot S \cdot t} \quad (3)$$

Where,

C_0 and C_t are MPc concentrations before and after illumination, respectively,

V is the reaction volume,

N_A is Avogadro constant,

S is the irradiated cell,

t is the irradiation time.³⁷

3. Result and Discussion

3.1. Chemistry

A metal ion in the core of a metallophthalocyanine could be active as a catalyst/photocatalyst. For photocatalytic activities of MPcs, it should contain metal ions, such as Mg (II), Al (III), Si (IV) and Zn (II), with a closed p or d electron configuration, resulting in a highly excited state life time. However, metal phthalocyanines with redox active metal ions, like Co (II) and Fe (II), having an open shell structure, show catalytic and electrocatalytic properties.^{38, 39}

Pcs containing four chalcone groups at peripherals were prepared using zinc (II) and cobalt (II) acetate salts (Scheme 1). The synthesis was initiated by reacting 4-hydroxybenzaldehyde with benzyl chloride in DMF in the presence of potassium carbonate as a base, which yielded 4-(benzyloxy)benzaldehyde **1** as a sole product in 87%.⁴⁰ Condensation of **1** and 4-hydroxyacetophenone in a mixture of EtOH and SOCl₂ gave the conjugated system, (*E*)-3-(4-(benzyloxy)phenyl)-1-(4-hydroxyphenyl)prop-2-en-1-one **2**.^{20, 38-41} Nucleophilic substitution reaction between **2** and 4-nitrophthalonitrile was performed in DMF, using potassium carbonate as a base at 50 °C for 24 hours under nitrogen atmosphere to afford the donor compound **3** in 76% yield.⁴² Syntheses of phthalocyanine derivatives **4a** and **4b** (Scheme 2) were performed at 130 °C, using Zn and Co metal salts under nitrogen atmosphere in DMF in the presence of DBU as a catalyst.⁴³ and achieved in good yields (43 and 53%).

The selection of metal atoms, i.e. Zn and Co, was made considering intramolecular donor-acceptor interaction between the soluble ligand and the terminal metal valence shells in phthalocyanine complexes. Thus, the final Pcs had good solubility properties obtained through the presence of conjugated systems at the peripherals. They were characterized by using UV-Vis, FT-IR, ¹H NMR, ¹³C NMR, and MALDI-TOF mass spectra.

Details of the structure elucidation of compounds **1-2** was discussed in supporting information file to avoid repetition of the literature.

IR spectra of compound **3** (Figure 1, (Figure S13).) demonstrated an aromatic C-H band at 3073 cm⁻¹ and an aliphatic C-H vibration band at 2931 cm⁻¹. A characteristic C≡N-vibration band of phthalonitrile appeared at 2232 cm⁻¹. While a C=O band was observed at 1655 cm⁻¹, aromatic C=C bands appeared at 1599 cm⁻¹ and 1588 cm⁻¹. Moreover, a band between 1140-1242 cm⁻¹ was attributed to C-O-C moiety.

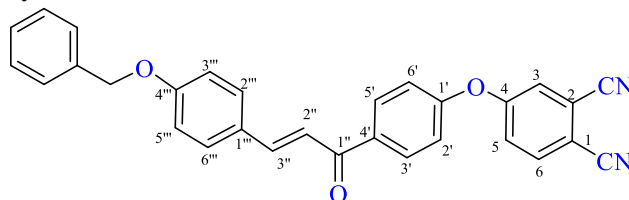
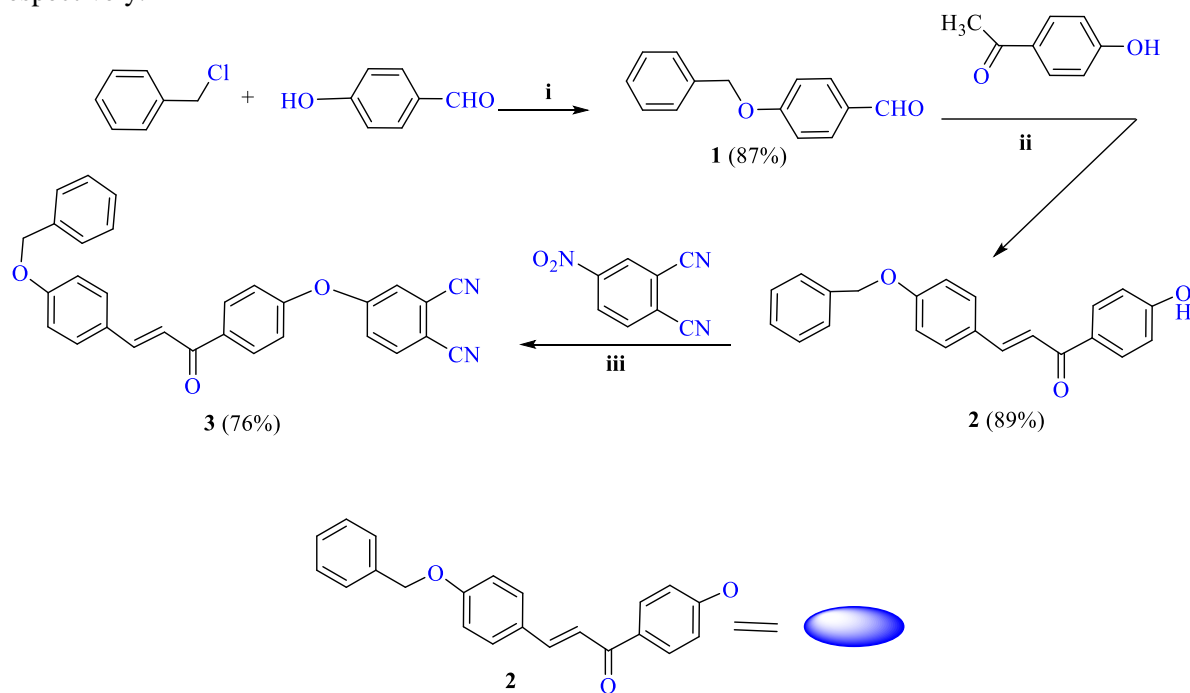


Figure 1. (*E*)-4-(4-(3-(4-(benzyloxy)phenyl)acryloyl)phenoxy)phthalonitrile **3**

Regarding the ¹H NMR of the compound **3**, while H₃/H₅' resonated as an AA' part of AA' BB' system giving quasi doublet at 8.19 ppm, H₃'' resonated by giving doublet ($J=15.0$ Hz) at 7.84 ppm

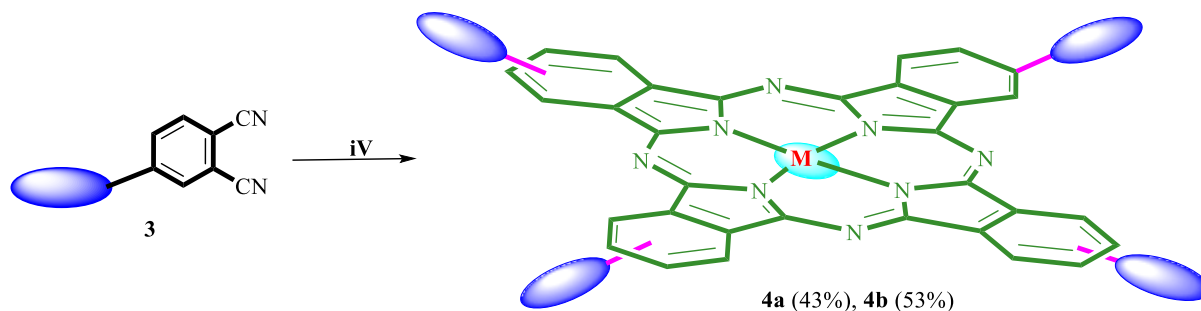
overlapping with H₆ at 7.80 ppm. H₂'/H₆' were seen as AA' part of AA' BB' system at 7.63 ppm. 5 ArH of phenyl ring, H₃, H₅, H₂'', resonated as multiplets at 7.55-7.25 ppm (PhCH₂O protons resonated as singlet at 5.19 ppm (Figure S7 and Figure S11). The ¹³C-NMR resonance signals were in agreement with structure (Figure S8-S10).

Although zinc phthalocyanine **4a** looked soluble in common organic solvents, its NMR measurements could not be performed due to aggregation, leading to broadening of the proton signals. Also, the NMR measurements of the cobalt phthalocyanine **4b** was precluded owing to its paramagnetic nature.^{20,41} In the electronic absorption spectrum, two absorption bands were observed for the phthalocyanine compounds, which are B and Q bands at about 300-450 and 600-700 nm, respectively.



Scheme 1. Synthetic route of compounds **1**, **2**, **3**. (i) K₂CO₃, DMF, rt; (ii) SOCl₂, EtOH, r.t., 12 h; (iii) K₂CO₃, DMF, 50 °C.

The phthalocyanines developed herein are well soluble in different solvents such as dichloromethane (DCM), *N,N*-dimethylformamide (DMF), tetrahydrofuran (THF) and dimethyl sulfoxide (DMSO). Moreover, they have low aggregation in these solvents and demonstrate characteristic absorption bands, i.e. a B-band between 360-385 nm and a Q-band band between 580-700 nm (Figure 4 and Figure 5). The UV-Vis spectra of the phthalocyanine derivatives **4a** and **4b** are good indication for their structures. Regarding the IR peaks of **4a** and **4b** (Figure S16 and Figure S19, respectively), while the characteristic functional group vibration of -CN (2232 cm⁻¹) were disappeared, appearance of the stretching vibration bands of C=O groups at 1594 cm⁻¹ (for Pc **4a**), and 1593 cm⁻¹ (for Pc **4b**) confirmed both phthalocyanines. The characteristic C-O-C bands at 1162 cm⁻¹ for **4a**, and 1213 cm⁻¹ for **4b** are also good indications for the structures. The other weak absorption bands between 3064-2865 cm⁻¹ for **4a**, and between 3068 - 2930 cm⁻¹ for **4b** are the aromatic =C-H stretching bands for the substituted phthalocyanines. The mass spectra of phthalocyanine derivatives **4a** and **4b** supported the proposed molecular formula. Molecular ion peaks identified *m/z* [M]⁺ calcd. for C₁₂₀H₈₀N₈O₁₂Zn: 1891.38; found [M + H]⁺ 1891.17 for **4a** (Figure S15) and *m/z* [M]⁺ calcd. for C₁₂₀H₈₀N₈O₁₂Co: 1884.94; found [M + H]⁺ 1884.78 for **4b** (Figure S18).



Scheme 2. Synthetic route of compounds **4a** and **4b**. **4a** $\text{Zn}(\text{OAc})_2 \cdot 2\text{H}_2\text{O}$, DMF, 130 °C, 24 h; **4b** $\text{Co}(\text{OAc})_2 \cdot 4\text{H}_2\text{O}$, DMF, 130 °C, 24 h

UV-Vis spectra of the compounds **4a** and **4b** were recorded in DMSO, DCM and DMF (Figures 2 and 3, respectively). The λ_{max} values for B and Q bands performed in these solutions are given in the Tables 1 and 2.

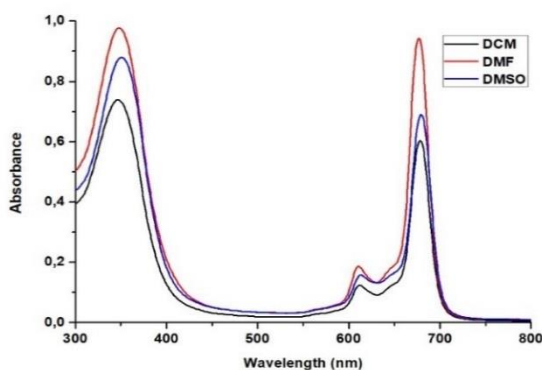


Table 1. The λ_{max} values of B and Q bands for **4a** performed in different solvents

| Solvent | λ_{max} , (nm) for B | λ_{max} , (nm) for Q ₁ | λ_{max} , (nm) for Q ₂ |
|---------|-------------------------------------|--|--|
| DMSO | 354 | 619 | 682.5 |
| DCM | 352.5 | 617.5 | 682 |
| DMF | 354.5 | 618 | 679.5 |

Figure 2. UV-Vis absorption spectra of: **4a** in different solvents (concentration = 1×10^{-5} M)

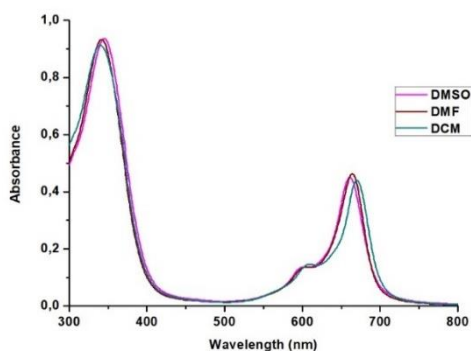


Table 2. The λ_{max} values of B and Q bands for **4b**

| Solvent | λ_{max} , (nm) for B | λ_{max} , (nm) for Q ₁ | λ_{max} , (nm) for Q ₂ |
|---------|-------------------------------------|--|--|
| DMSO | 359 | 601.5 | 664.5 |
| DCM | 345 | 610 | 674.5 |
| DMF | 345.5 | 602.5 | 667.5 |

Figure 3. UV-Vis absorptionspectra of: **4b** in different solvents (concentration = 1×10^{-5} M)

In different concentrations, the compound **4a** exhibited a low aggregation. Aggregation behavior of phthalocyanine **4a** in different concentrations depends on its skeleton and the solubility of chalcone groups in the peripheral position attached to this skeleton. Aggregation, which is usually exhibited as a coplanar association, varies according to peripheral or non-peripheral groups, solutions, concentrations and behaviours of the complexed metal ions.⁴³⁻⁴⁶

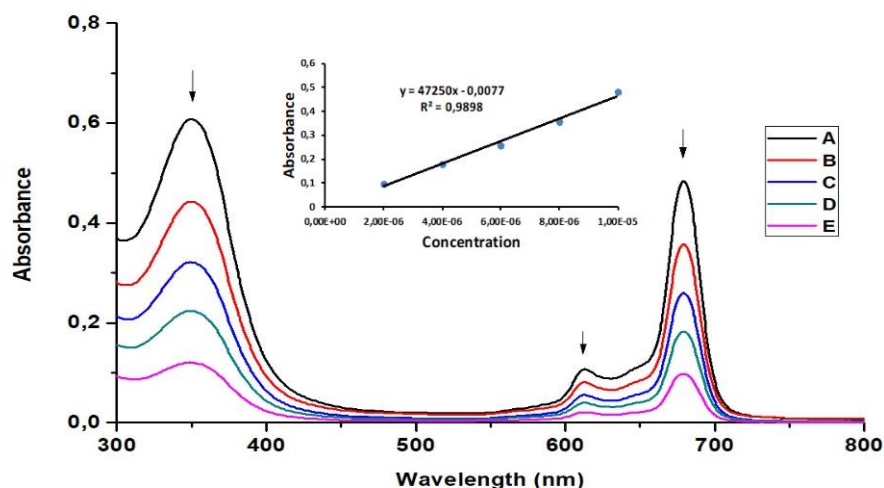


Figure 4. UV-Vis spectra of ZnPc **4a** in DMSO at different concentrations: 10×10^{-6} (A), 8×10^{-6} (B), 6×10^{-6} (C), 4×10^{-6} (D), 8×10^{-6} mol dm⁻³ (E). (inset: plot of absorbance versus concentration)

UV spectra of ZnPc **4a** in DMSO at different concentrations were examined for its aggregation behaviours (Figure 4). At lower concentrations (from 5×10^{-6} to 1×10^{-6}), the intensity of the Q-band absorption were decreased, and a new band did not form due to aggregation.⁴⁴

3.2. Metal Chelating Effects

Fe²⁺ has the ability to remove an electron from a peroxide resulting in the formation of a radical.²¹⁻²² In order to avoid radicals in metabolism, Fe²⁺ chelation might be a practicable therapeutic approach.²³ Divalent iron can quantitatively *chelates* ferrozine iron yielding a colored complex. The presence of another chelator can block the complex formation. In that case the color is diminished. Measurement of color changes allows the estimation of the chelating capacity of the chelator candidates.²³ Metal chelating activity of the phthalocyanines were determined at 25, 50, 75 and 100 μ M concentrations using their 1 mM stock solutions in DMSO.

Table 3. Ferrous ions chelating activity (%) of the phthalocyanines

| μ M ^a | 4a | 4b | EDTA ^c |
|----------------------|--------------------|--------------------|--------------------|
| 25 | 8.52 ± 0.18^b | 4.58 ± 0.31^b | 15.65 ± 0.15^b |
| 50 | 18.27 ± 0.22^b | 8.66 ± 0.28^b | 51.42 ± 0.18^b |
| 75 | 26.32 ± 0.17^b | 13.12 ± 0.42^b | 82.31 ± 0.08^b |
| 100 | 30.31 ± 0.31^b | 20.74 ± 0.24^b | 96.85 ± 0.21^b |

^a Four experiments were performed for all compounds in each experiment triplicated.

^b Mean values \pm SD are shown for triplicate experiments.

^c Reference compound.

Table 3 presents ferrous ions chelating activity (%) of **4a** and **4b**. For all studied samples, the chelation activity increased with the increase of their concentrations. **4a** was a good chelator and its chelation capacity increased from $8.52 \pm 0.18\%$ to $30.31 \pm 0.31\%$. **4a** and **4b** showed more or less ferrous ion chelation properties when compared with EDTA. Phthalocyanines with similar and higher metal chelating properties were reported in the literature^{21-22, 24} (Figure 5)

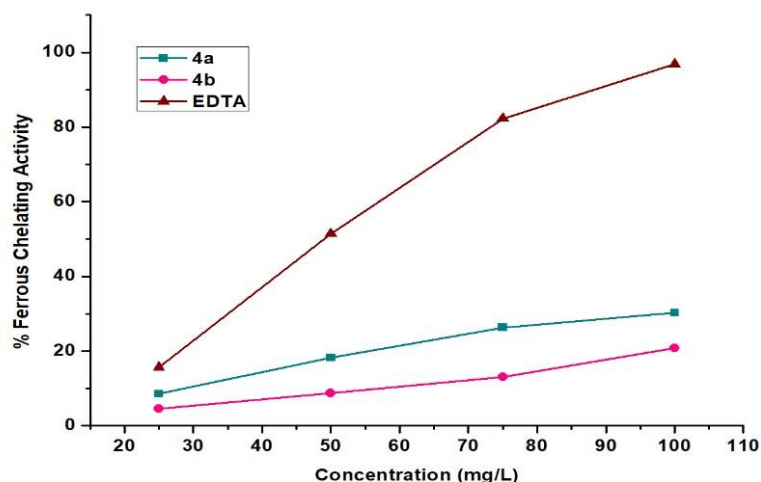


Figure 5. Ferrous chelating activity of **4a** and **4b** complex. The compounds were tested with concentrations ranging from 25 μ M to 100 μ M. EDTA was used as reference compound

3.3. DPPH Radical Scavenging Activity

This method is mainly based on reduction of 1,1-diphenyl-2-picrylhydrazyl (DPPH), which produces an easily identifiable strong violet color. The reduction of DPPH induces the radical to change color (violet to yellow) and this change is 517 nm.²⁵ DPPH radical scavenging assay is frequently used to detect the antioxidant capacity of synthesized compounds or plant extracts.^{21-22, 25-28} The ability of Pcs to scavenge DPPH radical were studied using above method. Pcs stock solutions in DMSO were treated with DPPH in methanol. Samples were used at different concentrations ranging from 25 to 100 μ M. DMSO was used as a control. DPPH radical scavenging capacity of Pcs are presented in Table 4. **4a** and **4b** exhibited DPPH radical scavenging capacity at studied concentrations (**4a**: 16.85 \pm 0.32%, 23.88 \pm 0.16%, 29.74 \pm 0.38%, 39.65 \pm 0.34% and **4b**: 8.62 \pm 0.27%, 14.41 \pm 0.37%, 29.45 \pm 0.52%, 34.99 \pm 0.36%). The highest antioxidant activity was observed with **4a** complex 25 μ M, 50 μ M, 75 μ M and 100 μ M. **4b** complex was not as effective as gallic acid²⁴ (Figure 6).

Table 4. Radical-scavenging activity on DPPH radicals (%) of the phthalocyanines.

| μ M ^a | 4a | 4b | Gallic Acid ^c |
|----------------------|-------------------------------|-------------------------------|-------------------------------|
| 25 | 16.85 \pm 0.32 ^b | 8.62 \pm 0.27 ^b | 68.88 \pm 0.40 ^b |
| 50 | 23.88 \pm 0.16 ^b | 14.41 \pm 0.37 ^b | 81.53 \pm 0.42 ^b |
| 75 | 29.74 \pm 0.38 ^b | 29.45 \pm 0.52 ^b | 87.71 \pm 0.38 ^b |
| 100 | 39.65 \pm 0.34 ^b | 34.99 \pm 0.36 ^b | 90.58 \pm 0.50 ^b |

^a Four experiments were performed for all compounds in each experiment triplicated.

^b Mean values \pm SD are shown for triplicate experiments.

^c Reference compound.

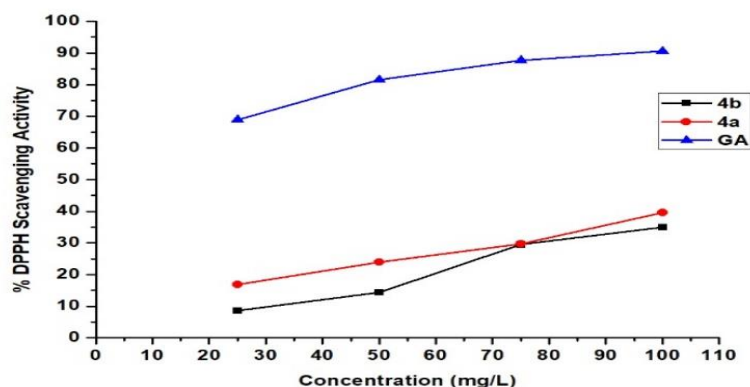


Figure 6. Radical-scavenging activity on DPPH radicals (%) of **4a** and **4b** complex. The compounds were tested with concentrations ranging from 25 μM to 100 μM . Gallic acid (GA) was used as standard mixtures

3.4. Photochemical Studies

3.4.1. Singlet Oxygen Quantum Yield (Φ_A)

To a 1×10^{-5} M zinc complex of **4a** in DMSO was added 1,3-Diphenylisobenzofuran (DPBF) for singlet oxygen quantum yield measurement as an extinguisher in dark. An 8.15×10^{15} photon $\text{s}^{-1}\text{cm}^{-2}$ was sent to the mixture every 10 seconds. The changes in absorption at 417 nm were then observed (Figure 7). A decrease of B band was observed. The calculated Φ_A was found to be high compare with the literature³⁰ (Table 5). These results indicated that **4a** could be used as a photosensitizer in PDT applications.

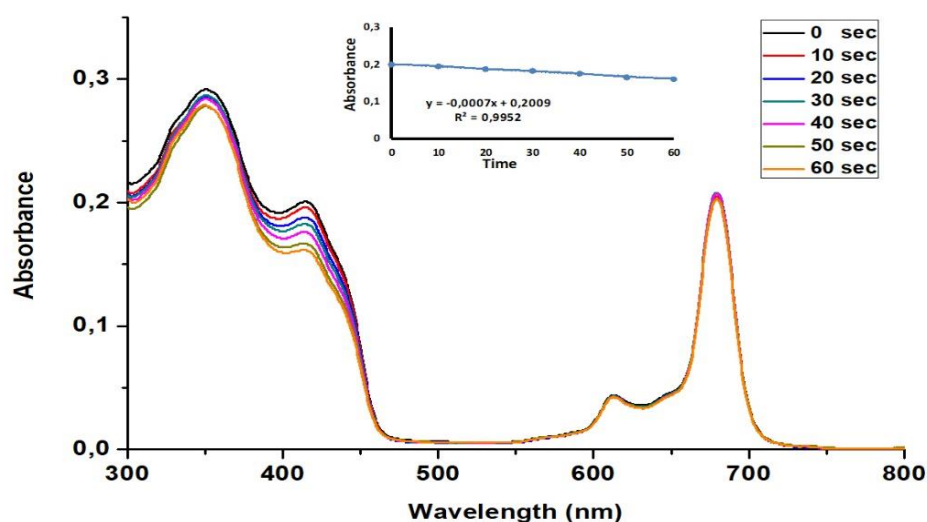


Figure 7. A typical spectrum for the determination of singlet oxygen quantum yield of **4a** in DMSO using DPBF as the singlet oxygen quencher. Concentration = 1×10^{-5} mol dm^{-3} . (Inset: plots of DPBF absorbance vs. time)

3.4.2. Photodegradation and Quantum Yield (Φ_d)

Production of singlet oxygen begins with absorption of a photon at 290-700 nm. Energy of this photon is then transmitted to the electrons in the molecule by converting it to a singlet oxygen, a

highly reactive form of triplet oxygen. While the molecule is transformed from its basic state into an excited state, it causes formation of functional groups (carbonyl, carboxyl, peroxide, etc.) and new conjugated bonds as well as configuration changes (dehydrogenation, demethylation, dehydromethylation) in the molecule. Moreover, when phthalocyanines are exposed to photons, different reactions may form. If a phthalocyanine contains an acceptor group, it is hardly oxidized, thus, photodegradation reaction slows down.

The compound **4a**, in DMSO, was exposed to UV-Vis light at 682.5 nm for photodegradation. Then, quantum yield in a specific time interval of 3.26×10^{16} photon $s^{-1}cm^{-2}$, and the changes in the Q band were examined (Figure. 8). During the photodegradation measurements Q band was observed to decrease over time, i.e. measured every 5 minutes. In line with the literature reports, both photodegradation and quantum yield values of **4a** increased (Table 5).³³ The compounds having photodegradation values in the range of 10^{-3} to 10^{-6} are not considered to be stable, according to the literature.

Table 5. Photochemical parameters of **4a** in DMSO

| Compound | Φ_A | Φ_d |
|-------------------|----------|----------------------|
| 4a | 0.80 | 5.7×10^{-4} |
| ZnPc ^a | 0.67 | 2.6×10^{-5} |

^aData from Ref.³⁹

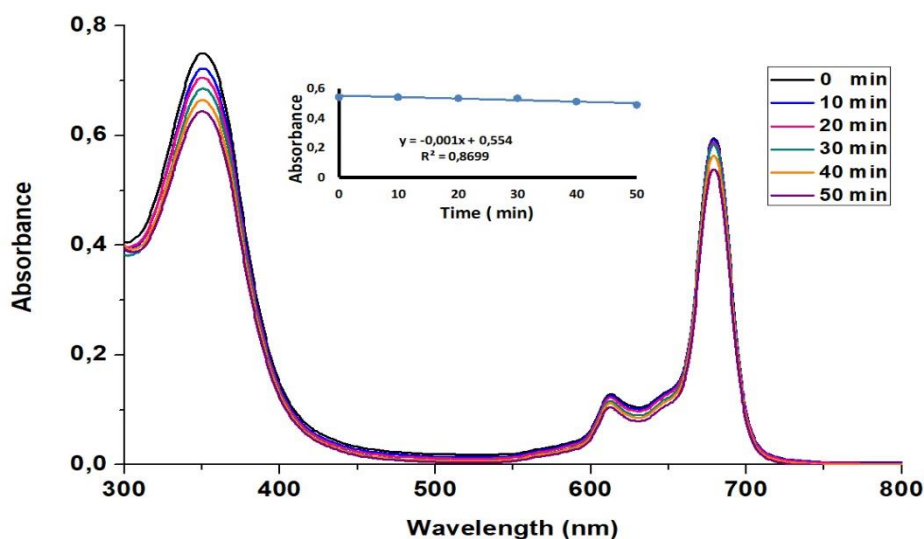


Figure 8. The photodegradation of **4a** in DMSO showing the disappearance of the Q band and the appearance of the reduction band from 0 min to 50 min (Inset: plot of Q band absorbance versus time)

4. Conclusions

In this study, two new phthalocyanines, substituted with chalcone bearing conjugated phenyloxy group, designed, synthesized and characterized. The starting material, 4-(benzyloxy)benzaldehyde **1**, was prepared from 4-hydroxy benzaldehyde and benzyl chloride in the presence of K_2CO_3 in DMF. In the second step, 4-(benzyloxy)benzaldehyde and 4-hydroxyacetophenone were reacted using $SOCl_2$ in absolute ethanol to give (*E*)-3-(4-(benzyloxy)phenyl)-1-(4-hydroxyphenyl)prop-2-en-1-one **2**. The nucleophilic substitution reaction between compound **2** and 4-nitrophthalonitrile were afforded compound **3** in DMF using potassium carbonate as the third step. Then ZnPc **4a** and CoPc **4b** were obtained as soluble compounds in good yields. Their photophysical and photochemical properties were investigated along with their biological and metal chelating effects and DPPH radical scavenging assays.

Conflict of interest

The authors confirm that this article content has no conflict of interest.

Acknowledgments

This work was supported, with Grand No: TBAG-113Z699, KBAG-115Z446, and 217Z043 by Scientific and Technological Research Council of Turkey (TUBITAK) respectively. Therefore, the authors are grateful for carrying out this research with the help of TUBITAK.

ORCID

Arif Baran: [0000-0002-4117-5099](https://orcid.org/0000-0002-4117-5099)

Emel Karakılıç: [0000-0002-8447-2851](https://orcid.org/0000-0002-8447-2851)

Özlem Faiz: [0000-0003-2447-0763](https://orcid.org/0000-0003-2447-0763)

Furkan Özen: [0000-0002-4703-0333](https://orcid.org/0000-0002-4703-0333)

References

- [1] Claessens, C. G.; Hahn, U.; Torres, T. Phthalocyanines: From outstanding electronic properties to emerging applications. *Chem. Record*, **2008**, *8*, 75-97.
- [2] Çakır, D.; Arslan, T.; Bıyıklıoğlu, Z. Effect of substituent position and metal type on the electropolymerization properties of chalcone substituted metallophthalocyanines. *Dalton Transaction*, **2015**, *44(48)*, 20859-20866.
- [3] Saka, E. T.; Çelik, G.; Sarkı, G.; Kantekin, H. Symmetrical and difunctional substituted cobalt phthalocyanines with benzoic acids fragments: Synthesis and catalytic activity *J. Incl. Phenom. Macrocycl. Chem.* **2016**, *85*, 161-168.
- [4] Stavric, B. Role of chemopreventers in human diet *Clin. Biochem.* **1994**, *27(5)*, 319-332.
- [5] Lu, J.; Wang, C. Medicinal components and pharmacological effects of *Rosa rugosa*. *Rec.Nat.Prod.* **1994**, *12*, 535-543.
- [6] Çarıkcı, S.; Kılıç, T.; Özer, Z.; Dirmenci, T.; Arabacı, T.; Gören, A.C. Quantitative determination of some phenolics in *Origanum laevigatum* Boiss. extracts via validated LC-MS/MS method and antioxidant activity. *J.Chem.Metrol.* **2018**, *12*, 121-127.
- [7] Miller, J. D.; Baron, E. D.; Scull, H.; Hsia, A.; Berlin, J. C.; McCormick, T.; Colussi, V.; Kenney, M. E.; Cooper, K. D.; Oleinick, N. L. Photodynamic therapy with the phthalocyanine photosensitizer Pc 4: The case experience with preclinical mechanistic and early clinical-translational studies. *Toxicol. Appl. Pharmacol.* **2007**, *224(3)*, 290-299.
- [8] Bacellar, I. O. L.; Tsubone, T. M.; Pavani, C.; Baptista, M. S. Photodynamic efficiency: From molecular photochemistry to cell death. *Int. J. Mol. Sci.* **2015**, *16(9)*, 20523-20559.
- [9] Dougherty, T. J.; Charles J. G.; Henderson B. W.; Jori, Giulio.; D, Kessel.; Korbek, M.; Moan J.; Qian, P. Photodynamic therapy. *J. Nat. Cancer Inst.* **1998**, *90(12)*, 889-905.
- [10] O'Connor, A. E.; Gallagher, W. M.; Byrne, A. T. Porphyrin and nonporphyrin photosensitizers in oncology: Preclinical and clinical advances in photodynamic therapy. *Photochem. Photobiol.* **2009**, *85*, 1053-1074.
- [11] Manashi, B.; Milnes, M.; Williams, C.; Balmoori, J.; Ye, X.; Stohsand, S.; Bagchi, D. Acute and chronic stress-induced oxidative gastrointestinal injury in rats, and the protective ability of a novel grape seed proanthocyanidin extract. *Nutr. Res.* **1999**, *19(8)*, 1189-1199.
- [12] Yıldız, S. Z.; Küçükislamoglu, M.; Tuna, M. Synthesis and characterization of novel flavonoid-substituted phthalocyanines using (\pm)naringenin. *J. Organomet. Chem.* **2009**, *694*, 4152-4161.
- [13] Acar, I.; Arslan, T.; Topçu, S.; Serkan, A. A.; Şen, S.; Serencam, H. Synthesis and electrochemistry of metallophthalocyanines bearing {4-[(2E)-3-(3,4,5-trimethoxyphenyl)prop-2-enoyl]phenoxy} groups. *J. Organomet. Chem.* **2014**, *752*, 25-29.
- [14] Formica, J. V.; Regelson, W. F. Review of the biology of quercetin and related bioflavonoids. *Chem Toxicol.* **1995**, *33(12)*, 1061-1080.
- [15] Alberto, M. E.; De Simone, B. C.; Mazzone, G.; Sicilia, E. Heavy atom effect on Zn(II) phthalocyanines derivatives: a theoretical exploration of the photophysical properties. *Phys. Chem.Phys.* **2015**, *17*, 23595.
- [16] Dumoulin, F.; Durmus, M.; Ahsen, V.; Nyokong, T. Synthetic pathways to water-soluble phthalocyanines and close analogs. *Coord. Chem. Rev.* **2010**, *254*, 2792-2847.
- [17] Mori, GD.; Fu, Z.; Viola, E.; Cai, X.; Ercolani, C.; Donzello, M.P.; Kadish, K. M. Tetra-2,3-pyrazinoporphyrazines with externally appended thienyl rings: Synthesis, UV-visible spectra,

- electrochemical behavior, and photoactivity for the generation of singlet oxygen. *Inorg. Chem.* **2011**, *50*, 8225–8237.
- [18] Cong, F.; Wei, Z.; Huang, Z.; Yu, F.; Liu, H.; Cui, J.; Yu, H.; Chu, X.; Du, X.; Xing, K.; Lai, Characteristic absorption band split of symmetrically tetra-octyloxy metal phthalocyanines. *J. Dyes Pigment.* **2015**, *120*, 1–7.
- [19] Fandakli, S.; Doğan, S.; Sellitepe, H.E.; Yaşar, A.; Yaylı N. Synthesis, theoretical calculation and α -glucosidase inhibition of new chalcone oximes. *Org. Commun.* **2018**, *215*, 23–34.
- [20] Ivanova, Y.; Gerova, M.; Petrov, O. $\text{SOCl}_2/\text{EtOH}$: Catalytic system for synthesis of chalcones. *Catal. Commun.* **2008**, *9*, 315–316.
- [21] Kantar, G. K.; Faiz, Ö.; Sahin, O.; Sasmaz, S. Phthalocyanine and azaphthalocyanines containing eugenol: synthesis, DNA interaction and comparison of lipase inhibition properties. *J. Chem. Sciences* **2017**, *129*, 1247-1256.
- [22] Li, M.; Pare, P.W.; Zhang, J.; Kang, T.; Zhang, Z.; Yang, D.; Wang, K.; Xing, H. Antioxidant capacity connection with phenolic and flavonoid content in Chinese medicinal herbs. *Rec. Nat. Prod.* **2018**, *12*, 239–250.
- [23] Halfon, B.; Çetin, Ö.; Kökdil, G.; Topçu, G. Chemical investigation and bioactivity screening of *Salvia cassia* extracts. *Rec. Nat. Prod.* **2019**, *13*, 156–166.
- [24] Baran, A.; Çol, S.; Karakılıç, E.; Özen, F. Photophysical, photochemical and DNA binding studies of prepared phthalocyanines. *Polyhedron* **2020**, *175*, 114205.
- [25] Pavithra, K.; Vadivukkarasi, S. Evaluation of free radical scavenging activity of various extracts of leaves from *Kedrostis foetidissima* (Jacq.) Cogn. *Food Sci. Human Wellnes.* **2015**, *4* (1), 42–46.
- [26] Kauthale, S.; Tekale, S.; Damal, M.; Sangshetti, J.; Pawar, R. Synthesis, antioxidant, antifungal, molecular docking and ADMET studies of some thiazolyl hydrazones. *Bioorg. Med. Chem. Lett.* **2017**, *27*(16), 3891–3896.
- [27] Zhou, D.Y.; Sun, Y. X.; Shahidi, F. Preparation and antioxidant activity of tyrosol and hydroxytyrosol esters. *J. Funct. Foods* **2017**, *37*, 66–73.
- [28] Carter, P. Spectrophotometric determination of serum Iron at the submicrogram level with a new reagent (Ferrozine). *Anal. Biochem.* **1971**, *40* (2), 450–458.
- [29] Blois, M.S. Antioxidant determination by the use of a stable free radical. *Nature* **1958**, *181*, 1199–1200.
- [30] Chamarthi, N.R.; Ponne, V.C.; Pulluru, H.B.; Balija, J.D.; Gutala, S.R.; Kallimakula, S.V.; Chinthu, V.; Wudayagiri, R. New symmetrical acyclic and alicyclic bisurea derivatives of 4,4'-methylenebis(phenyl isocyanate): Synthesis, characterization, bioactivity and antioxidant activity evaluation and molecular docking studies. *Org. Commun.* **2018**, *11*, 80-97.
- [31] Brannon, J.H. Picosecond laser photophysics. Group 3A phthalocyanines. *J. Am. Chem. Soc.* **1980**, *102*, 62-65.
- [32] Seotsanyana, M. I.; Kuznetsova, N.; Nyokong, T. Photochemical studies of tetra-2,3-pyridinoporphyrazines. *J. Photochem. Photobiol. A Chem.* **2001**, *140*, 215-222.
- [33] Spiller, W.; Kliesch, H.; Worhle, D.; Hackbarth, S.; Roder, B.; Schnurpfeil, G. Singlet oxygen quantum yields of different photosensitizers in polar solvents and micellar solutions. *J. Porphy. Phthal.* **1982**, 145–158.
- [35] Bayrak, R.; Akçay, H.T.; Pişkin, M.; Durmuş, M.; Değirmencioğlu, I. Azine-bridged binuclear metalphthalocyanines functioning photophysical and photochemical-responsive. *Dyes Pigment.* **2012**, *95*, 330–337.
- [36] Nyokong, T. Effects of substituents on the photochemical and photophysical properties of main group metal phthalocyanines. *Coord. Chem. Rev.* **2007**, *251*, 1707–1722.
- [37] Ogunsipe, A.; Nyokong, T. Photophysical and photochemical studies of sulphonated non-transition metal phthalocyanines in aqueous and non-aqueous media *J. Photochem. Photobiol. A Chem.* **2005**, *173*, 211–220.
- [38] Darwent, J. R.; Douglas, P.; Harriman, A.; Porter, G.; Richoux, M. Metal phthalocyanines and porphyrins as photosensitizers for reduction of water to hydrogen. *Coord. Chem. Rev.* **1982**, *44*, 83-126.
- [39] Zagal, J. H.; Gulppi, M, A.; Cardenas-Jiron, G. Metal-centered redox chemistry of substituted cobalt phthalocyanines adsorbed on graphite and correlations with MO calculations and Hammett parameters. Electrocatalytic reduction of a disulfide. *Polyhedron* **2000**, *19*, 2255-2260.
- [40] Somakala, K.; Amir, M.; Sharma, V.; Wakode, S. Synthesis and pharmacological evaluation of pyrazole derivatives containing sulfonamide moiety. *Monatsh. Chem.* **2016**, *147*, 2017–2029.
- [41] Shinohara, H.; Tsaryova, O.; Schnurpfeil, G.; Wöhrle, D. Differently substituted phthalocyanines: Comparison of calculated energy levels, singlet oxygen quantum yields, photo-oxidative stabilities, photocatalytic and catalytic activities differently substituted phthalocyanines: Comparison of calculated energy levels, singlet oxygen quantum yields, photo-oxidative stabilities, photocatalytic and catalytic activities. *J. Photochem. Photobiol. A Chem.* **2006**, *184*, 50–57.

- [42] Ozcesmeci, M.; Ozcesmeci, I.; Hamuryudan, E. Synthesis and characterization of new polyfluorinated dendrimeric phthalocyanines. *Polyhedron* **2010**, *29*, 2710–2715.
- [43] Hamuryudan, E.. Synthesis and solution properties of phthalocyanines substituted with four crown ethers. *Dyes Pigment.* **2006**, *2-3*, 151-157.
- [44] Durmus, M.; Nyokong, T.; Synthesis and solution properties of phthalocyanines substituted with four crown ethers. *Polyhedron* **2007**, *26*, 2767-2776.
- [45] Engelkamp, H.; Nolte, R. J. M. J. Doctoral thesis. *Porphyrins Phthal.* **2000**, *4*, 454.
- [46] Kobak, R. Z. U.; Gul, A. Synthesis and solution studies on azaphthalocyanines with quaternary aminoethyl substituents. *Color Technol.* **2009**, *125*, 22-28.

A C G
publications

© 2020 ACG Publications

Supporting Information

Org. Commun. 13:2 (2020) 65-78

Synthesis of chalcone-containing zinc and cobalt metallophthalocyanines; investigation of their photochemical, DPPH radical scavenging and metal chelating characters

Arif Baran^{1*}, Emel Karakılıç¹, Özlem Faiz² and Furkan Özen¹

¹*Department of Chemistry, Faculty of Arts and Sciences, Sakarya University,
54187, Sakarya, Türkiye*

²*Department of Chemistry, Faculty of Arts and Sciences, ²RTE University
53100, Rize, Türkiye*

| Table of Contents | Page |
|--|------|
| Figure S1: ¹ H NMR spectrum of compound 1 (in CDCl ₃) | 2 |
| Figure S2: ¹³ C NMR spectrum of compound 1 (in CDCl ₃) | 3 |
| Figure S3: FT-IR spectrum of compound 1 | 4 |
| Figure S4: ¹ H NMR spectrum of compound 2 (in CDCl ₃ / CD ₃ OD: 5/1) | 5 |
| Figure S5: ¹³ C NMR spectrum of compound 2 (in CDCl ₃ / CD ₃ OD: 5/1) | 6 |
| Figure S6: FT-IR spectrum of compound 2 | 7 |
| Figure S7: ¹ H NMR spectrum of compound 3 (in CDCl ₃) | 8 |
| Figure S8: ¹³ C NMR spectrum of compound 3 (in CDCl ₃) | 9 |
| Figure S9: DEPT NMR spectrum of compound 3 (in CDCl ₃) | 10 |
| Figure S10: APT NMR spectrum of compound 3 (in CDCl ₃) | 11 |
| Figure S11: COSY spectrum of compound 3 (in CDCl ₃) | 12 |
| Figure S12: HETCOR spectrum of compound 3 (in CDCl ₃) | 13 |
| Figure S13: FT-IR spectrum of compound 3 | 14 |
| Figure S14: UV-Vis spectrum of compound 4a (in DMF) | 15 |
| Figure S15: MALDI-TOF mass spectrum of compound 4a | 16 |
| Figure S16: FT-IR spectrum of compound 4a | 17 |
| Figure S17: UV-Vis spectrum of compound 4b (in DMF) | 18 |
| Figure S18: MALDI-TOF mass spectrum of compound 4b | 19 |
| Figure S19: FT-IR spectrum of compound 4b | 20 |
| S1: Structure Elucidation of Compounds 1-2 | 21 |

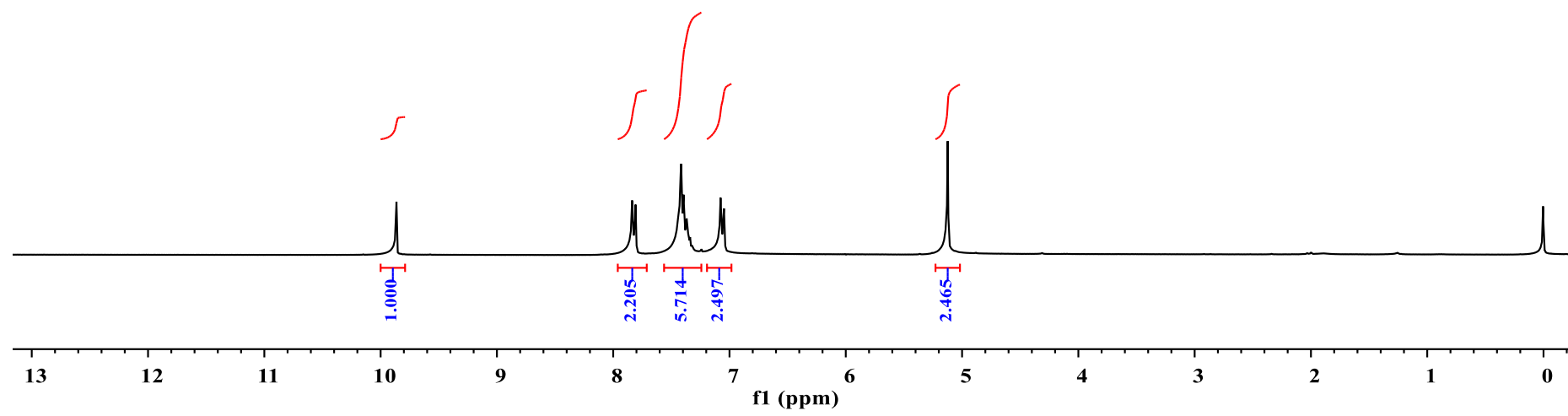
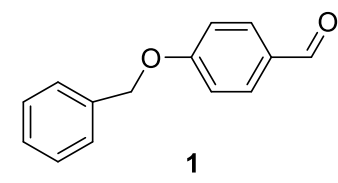
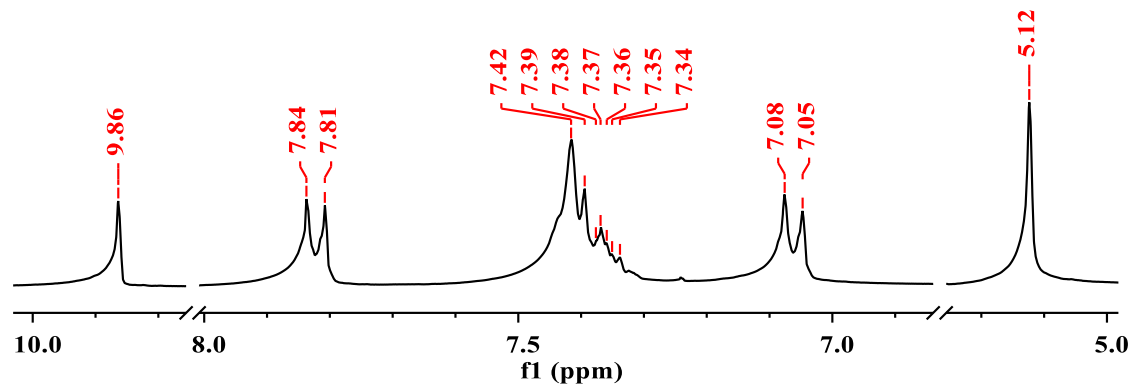


Figure S1: ¹H NMR spectrum of compound **1** in (CDCl₃)

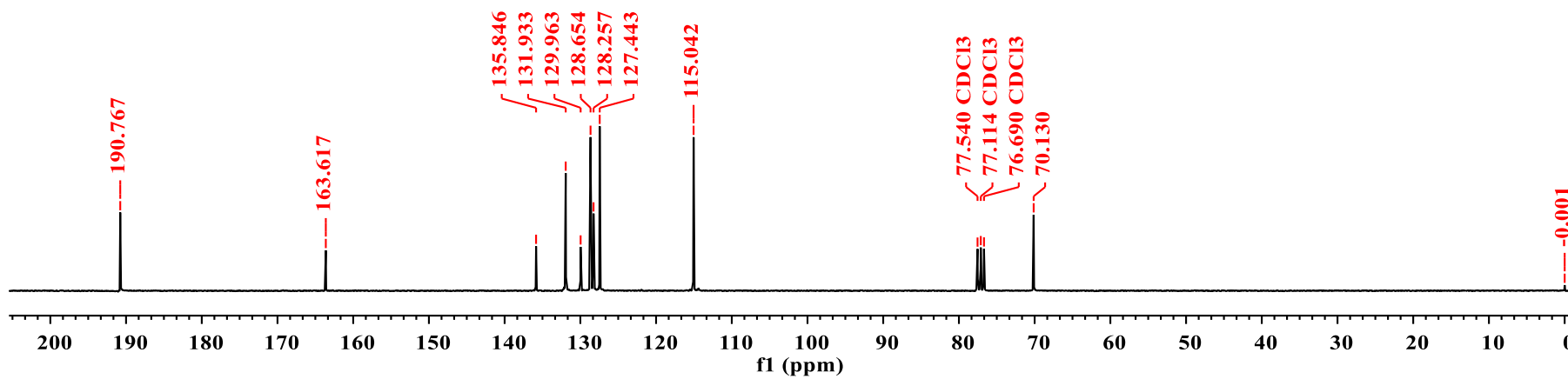
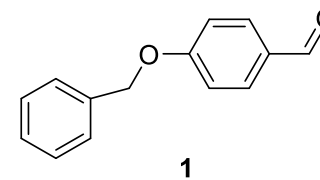
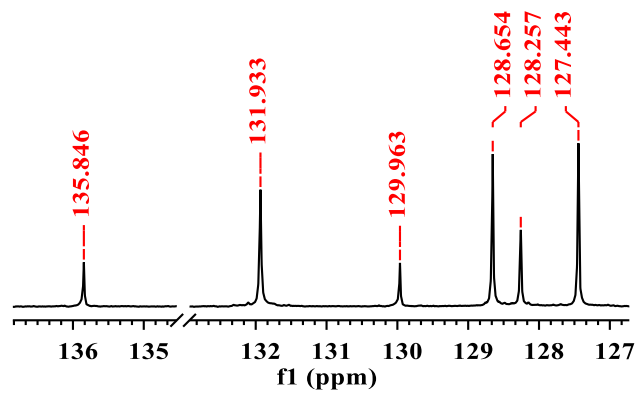


Figure S2: ^{13}C NMR spectrum of compound 1 (in CDCl_3)

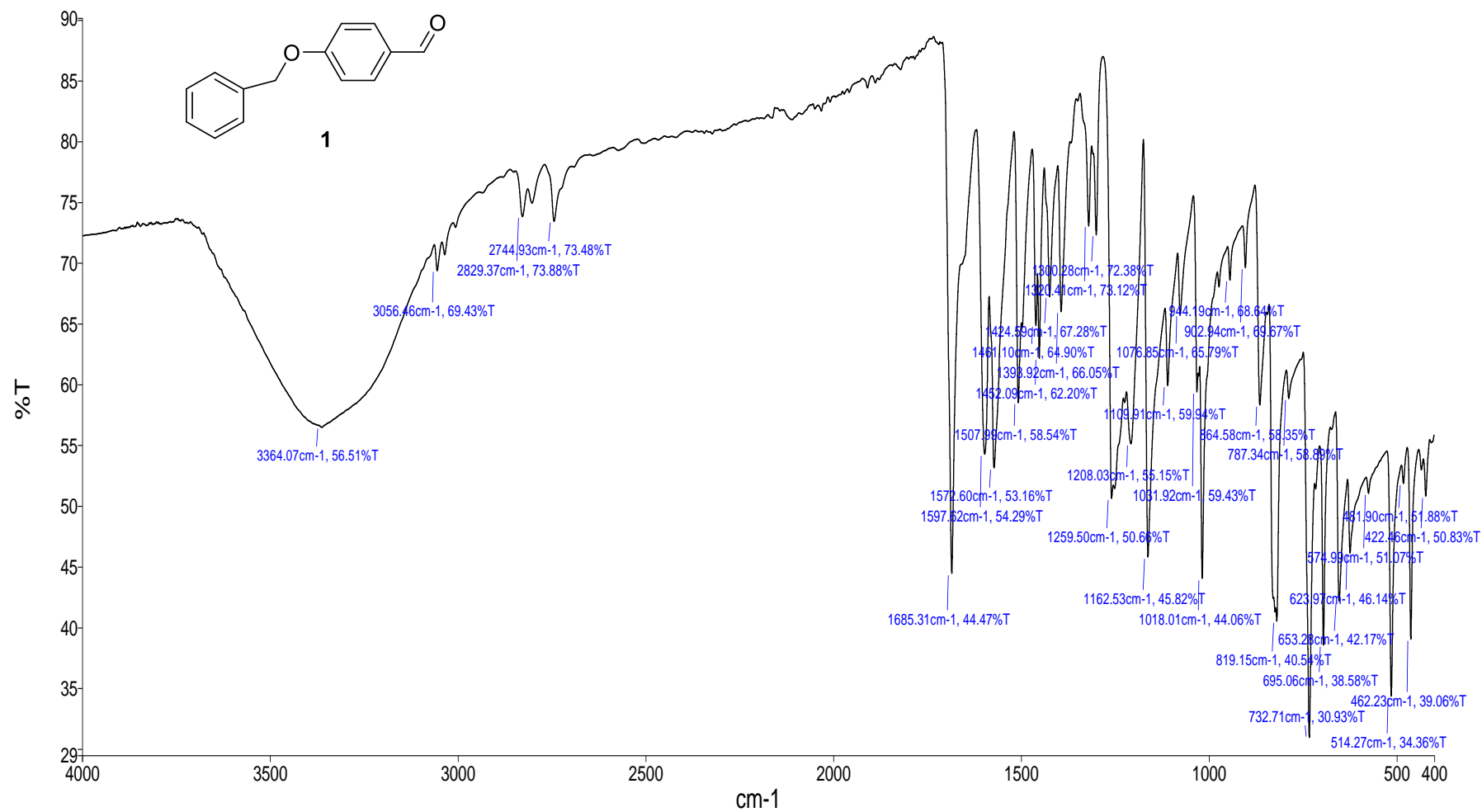
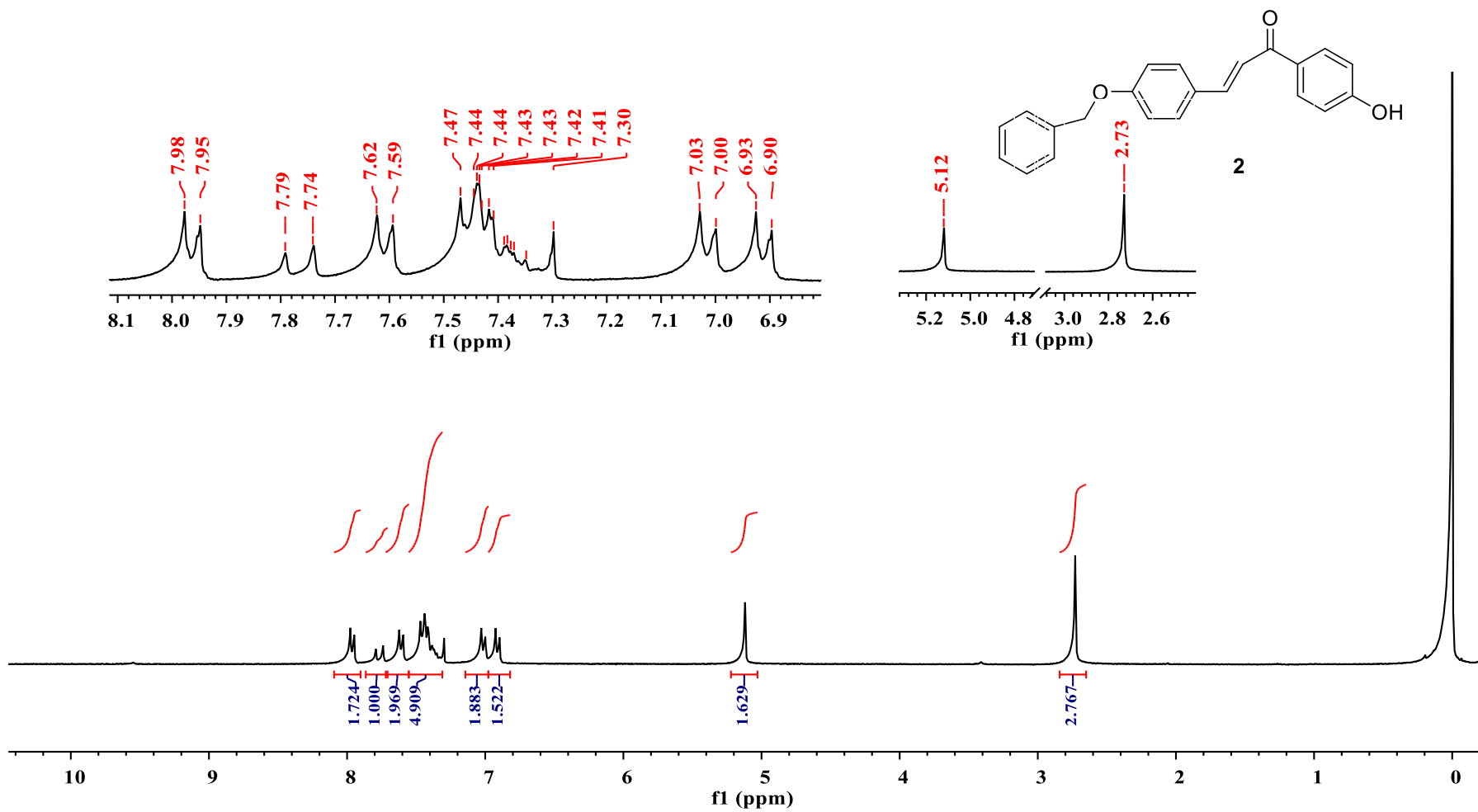


Figure S3: FT-IR spectrum of compound **1**

© 2020 ACG Publications. All rights reserved.



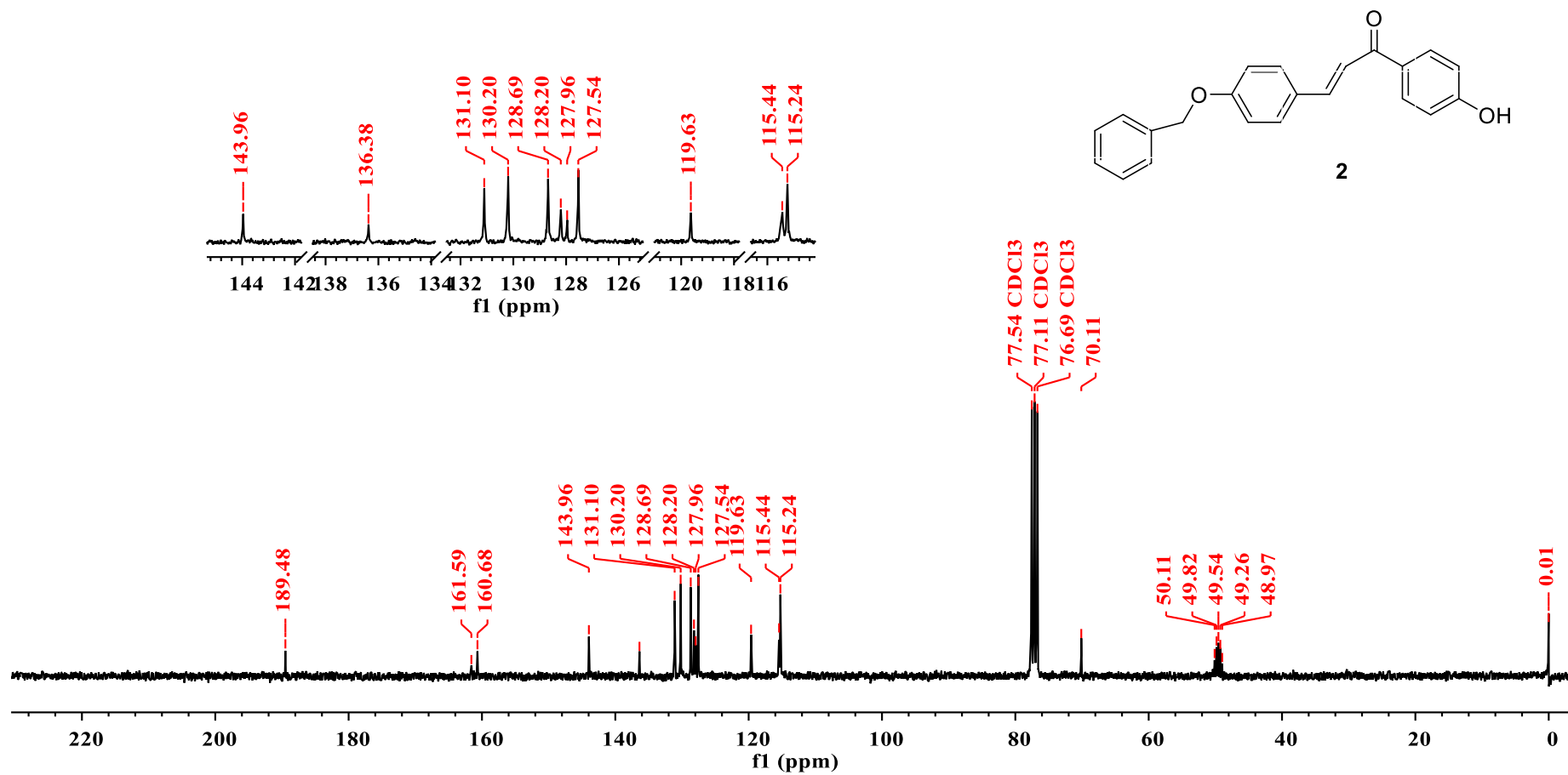


Figure S5: ¹³C NMR of spectrum of compound 2 (in CDCl₃/ CD₃OD: 5/1)

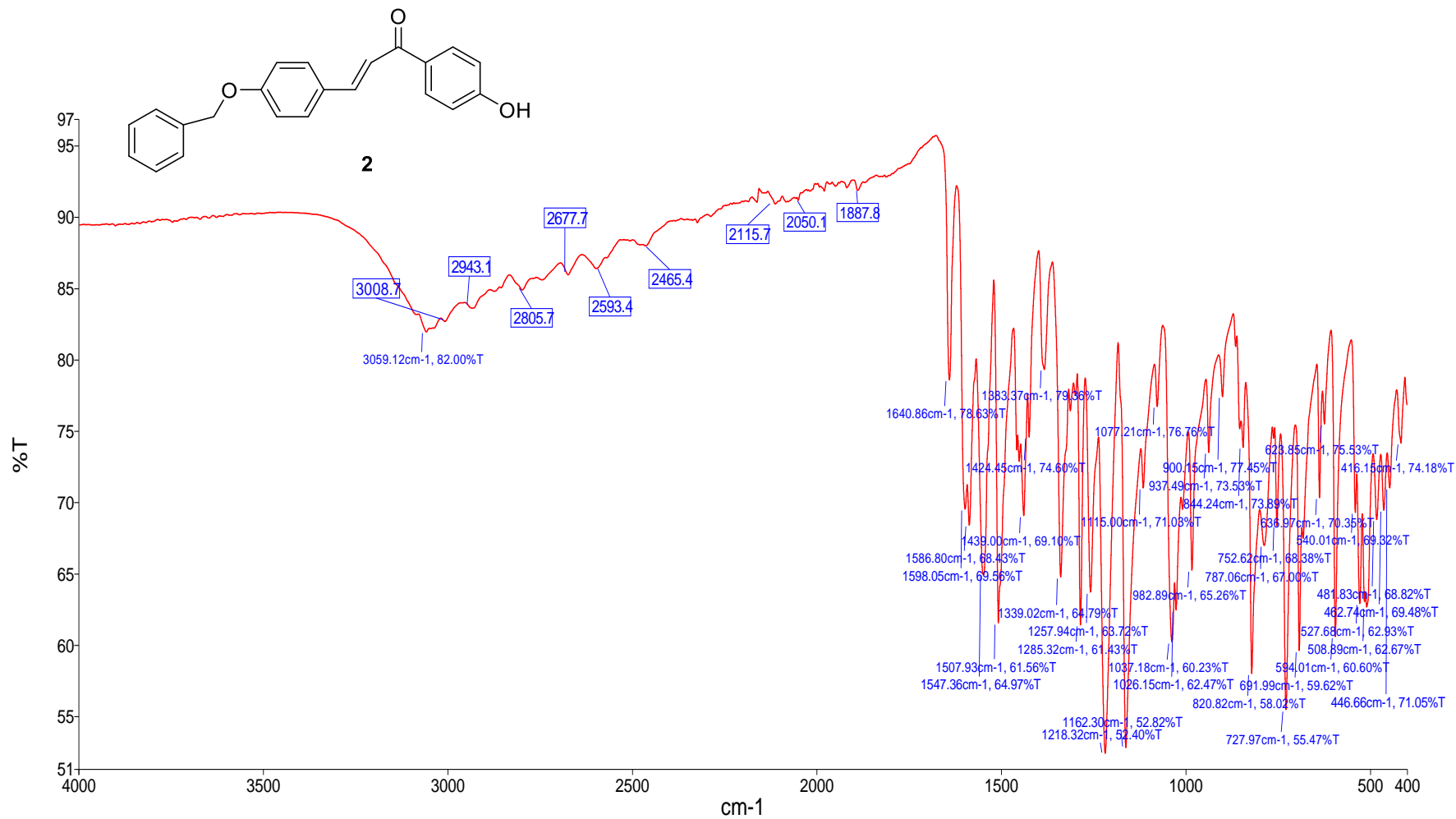


Figure S6. FT-IR spectrum of compound **2**

© 2020 ACG Publications. All rights reserved.

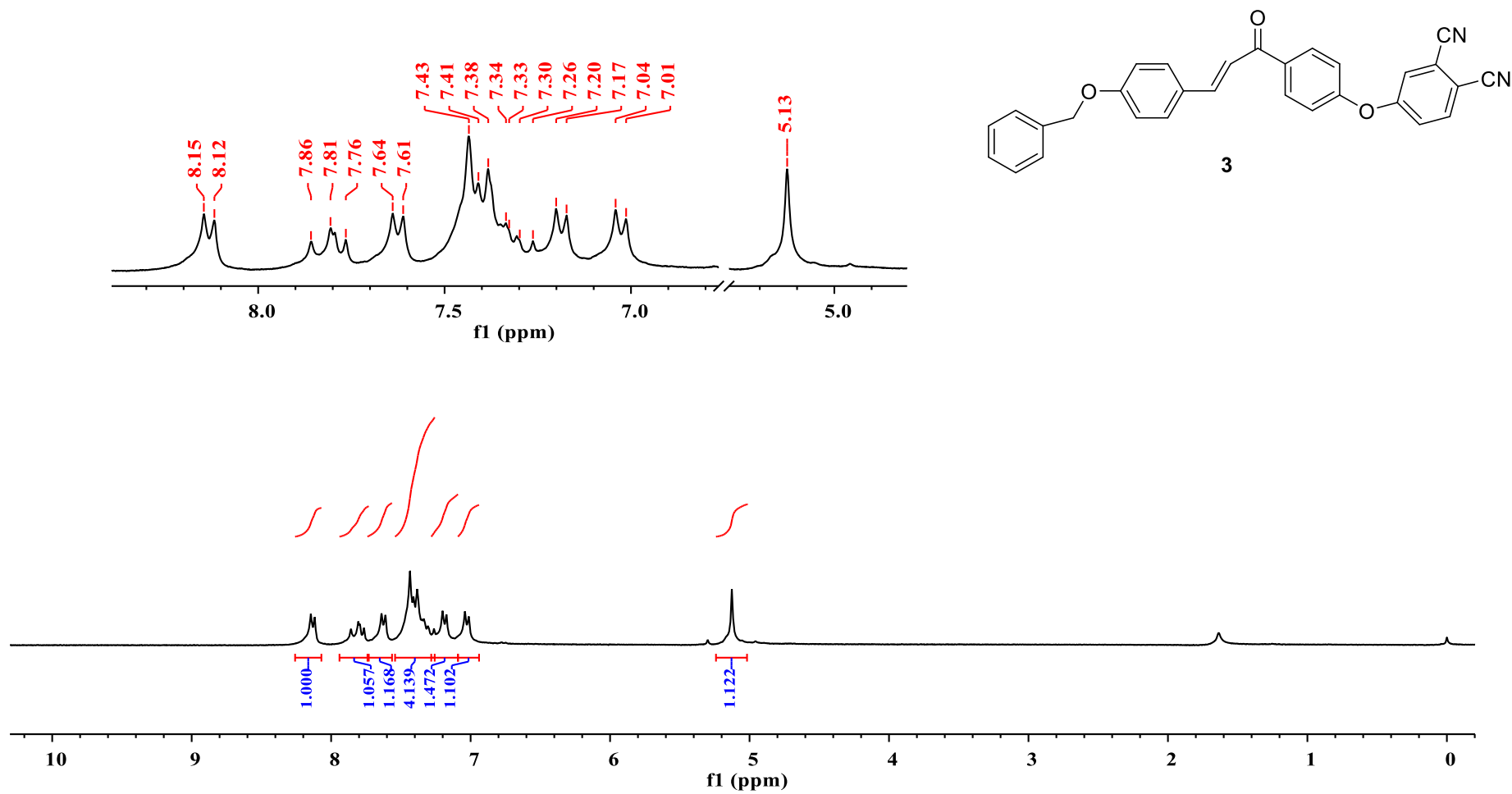


Figure S7: ¹H NMR spectrum of compound **3** (in CDCl₃)

© 2020 ACG Publications. All rights reserved.

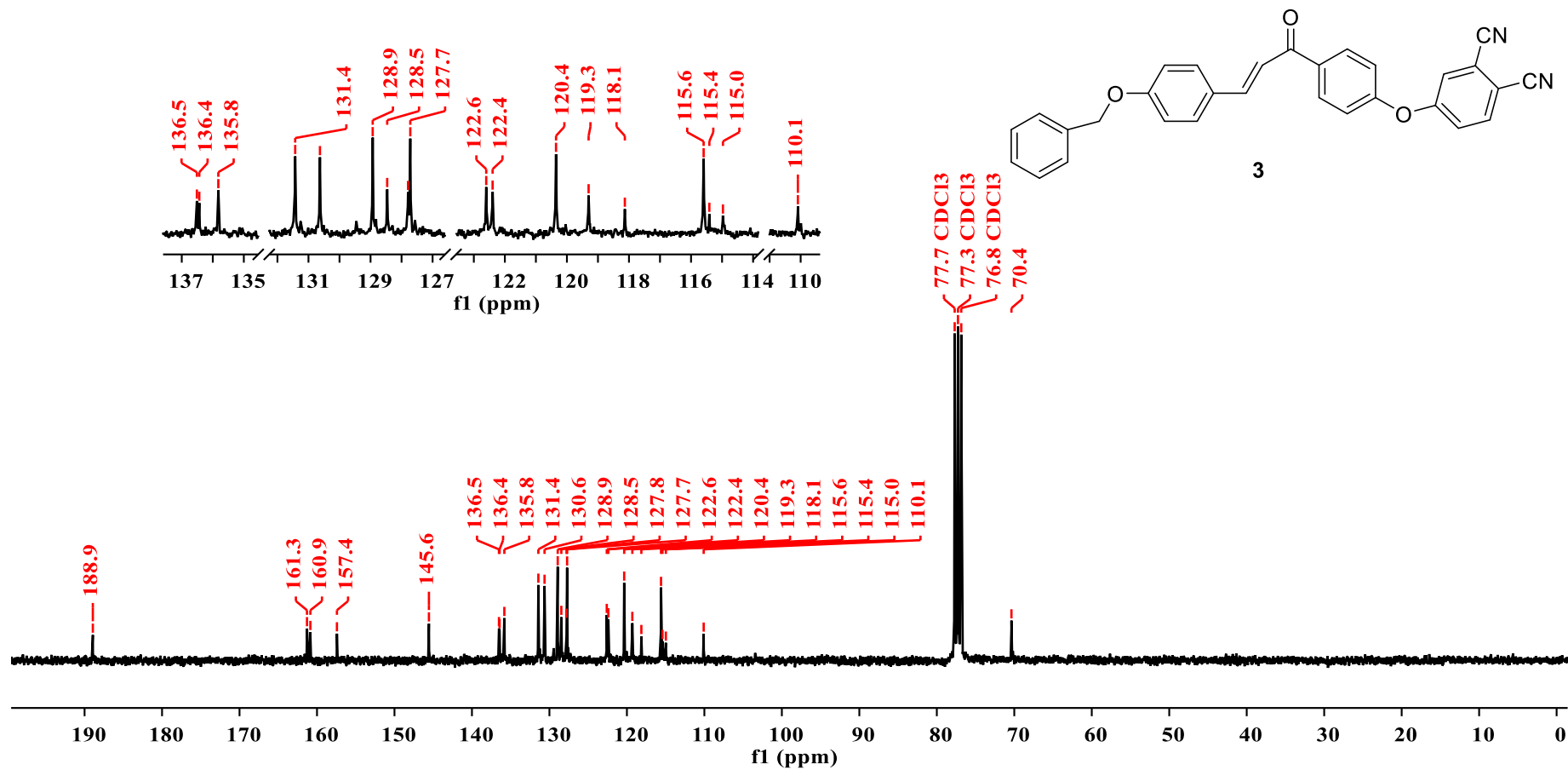


Figure S8: ^{13}C NMR of spectrum of compound **3** (in CDCl_3)

© 2020 ACG Publications. All rights reserved.

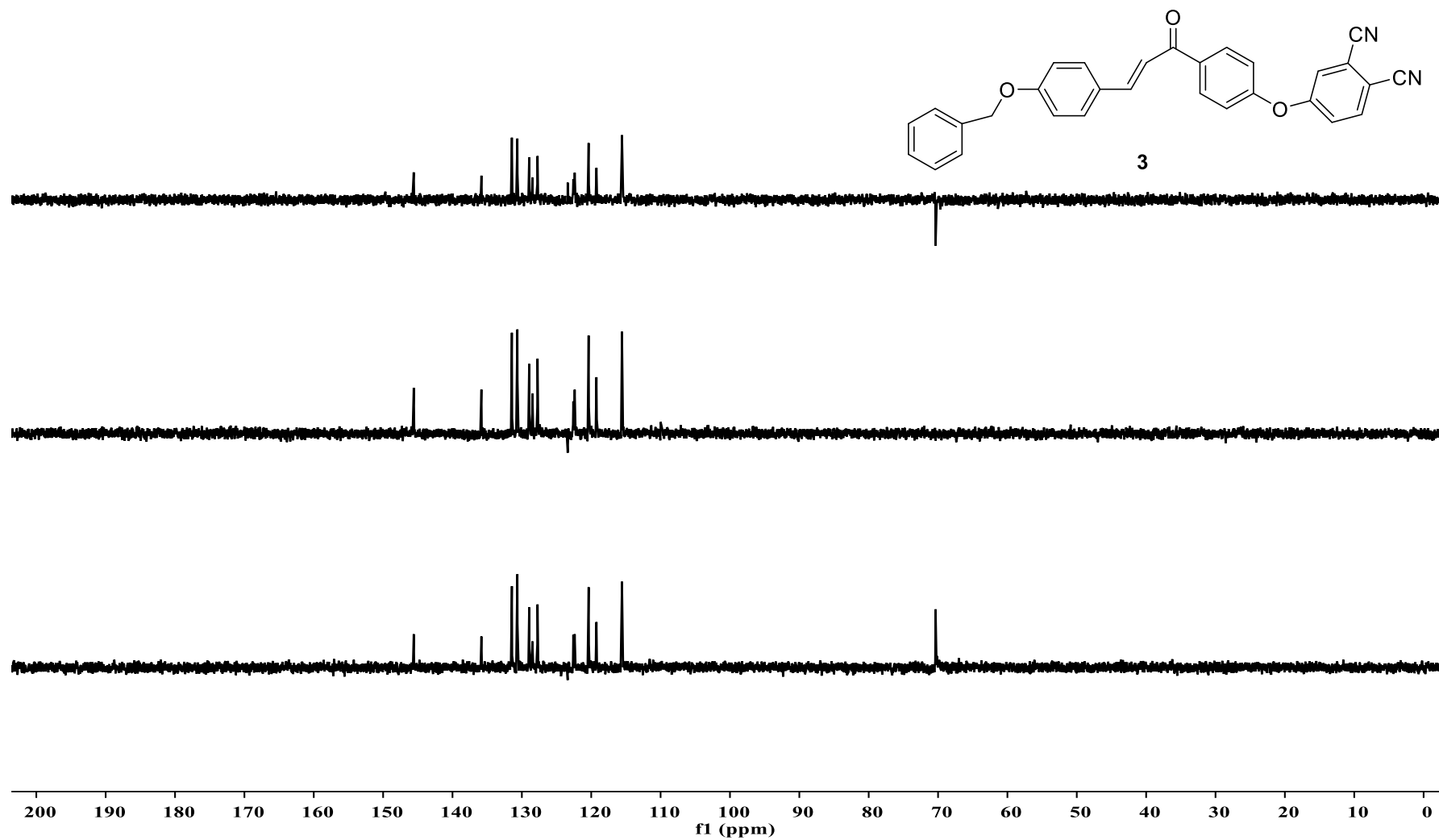


Figure S9: Dept NMR Spectrum of compound **3** (in CDCl₃)

© 2020 ACG Publications. All rights reserved.

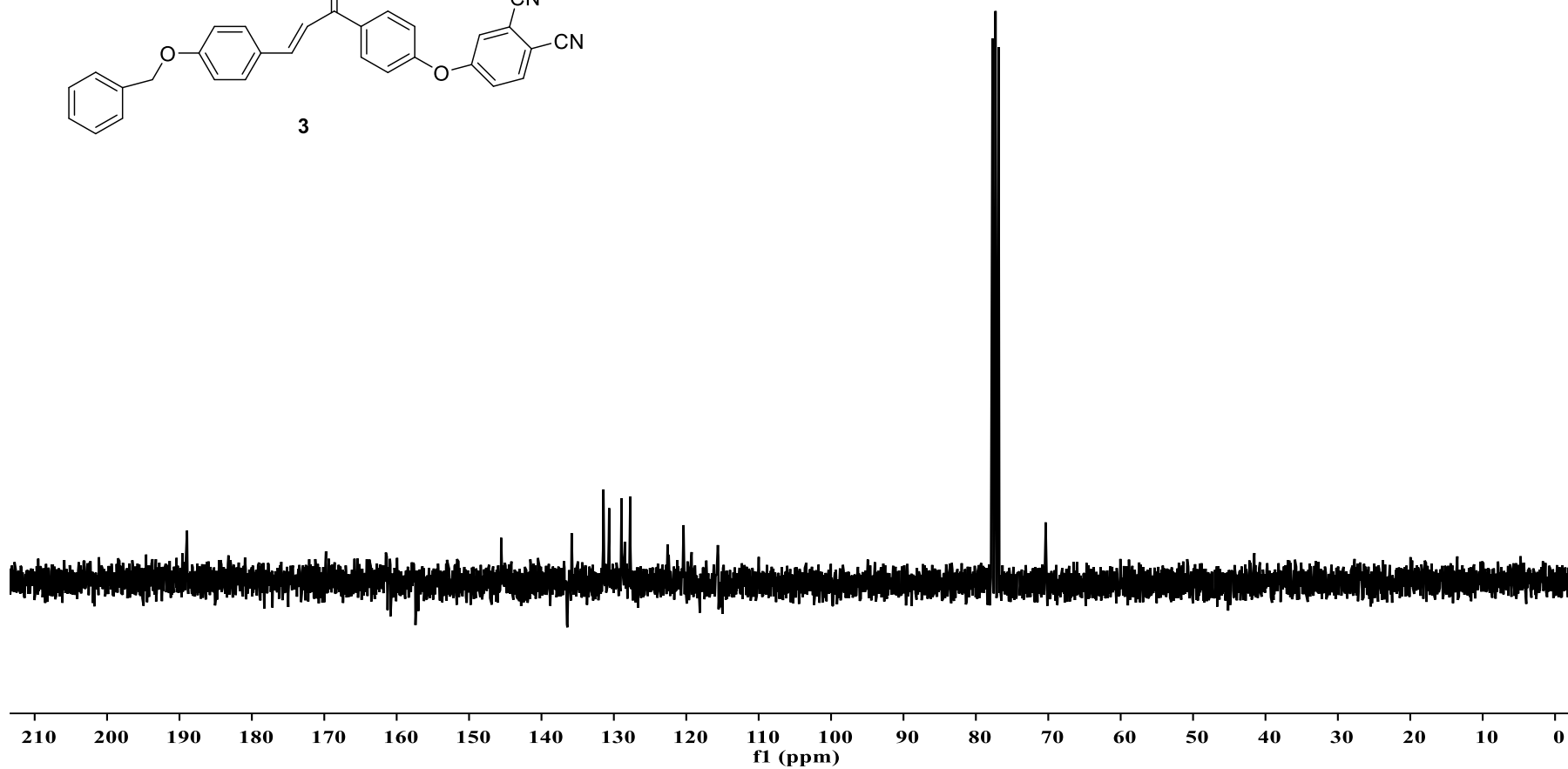
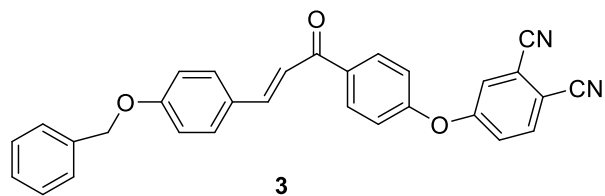


Figure S10: APT spectrum of compound **3** (in CDCl₃)

© 2020 ACG Publications. All rights reserved.

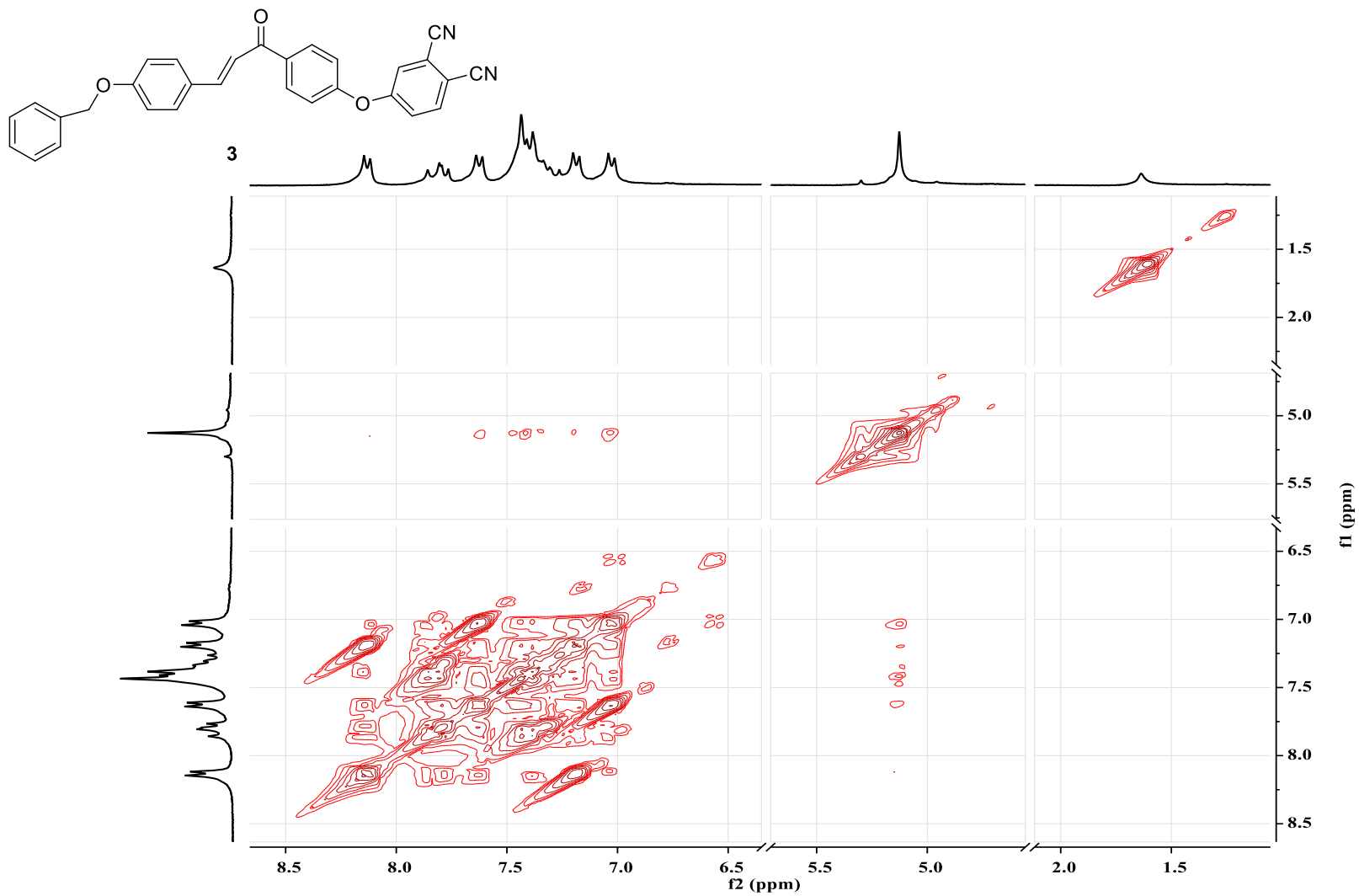


Figure S11: COSY spectrum of compound **3** (in CDCl₃)

© 2020 ACG Publications. All rights reserved.

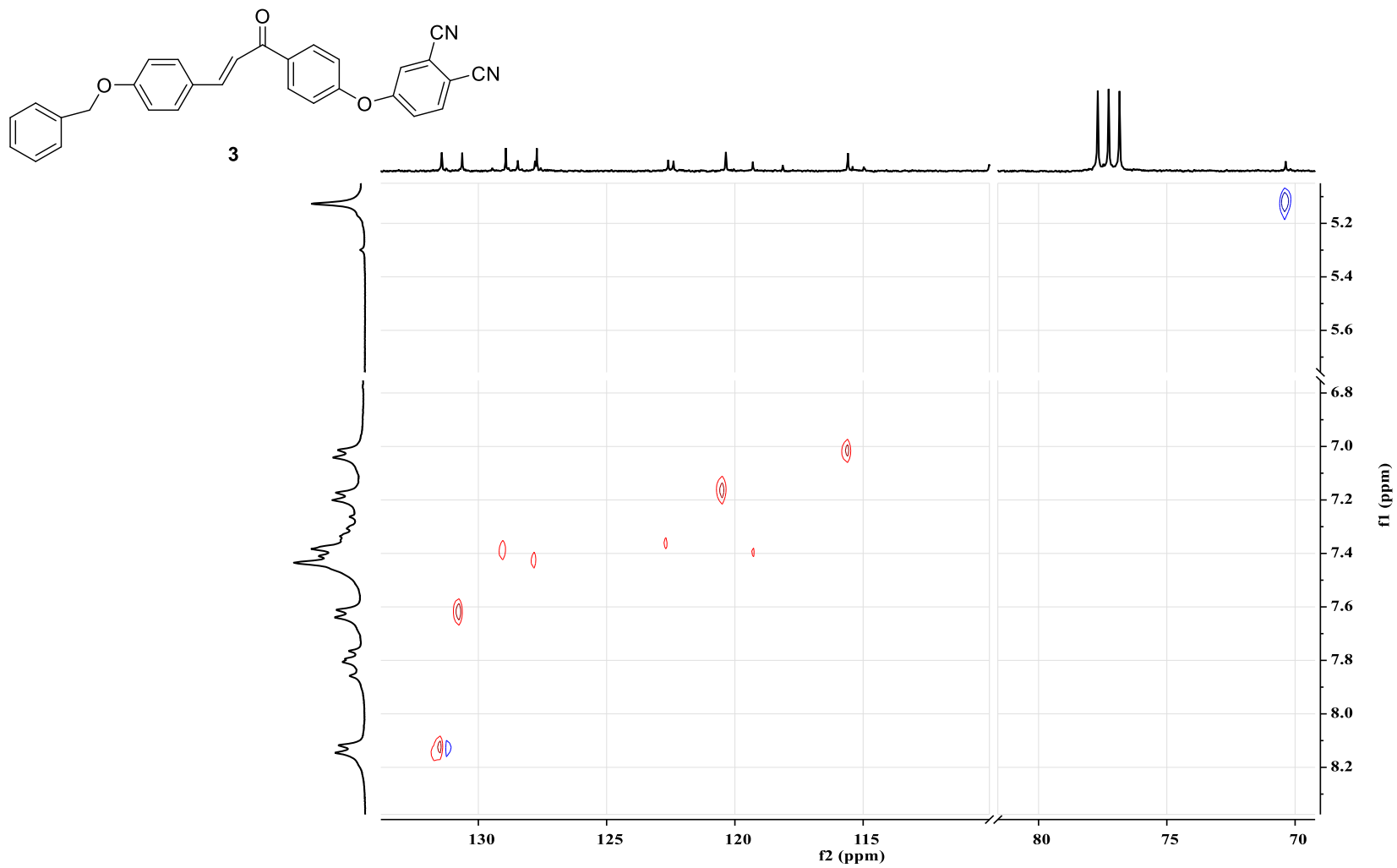


Figure S12: HETCOR spectrum of compound **3** (in CDCl₃)

© 2020 ACG Publications. All rights reserved.

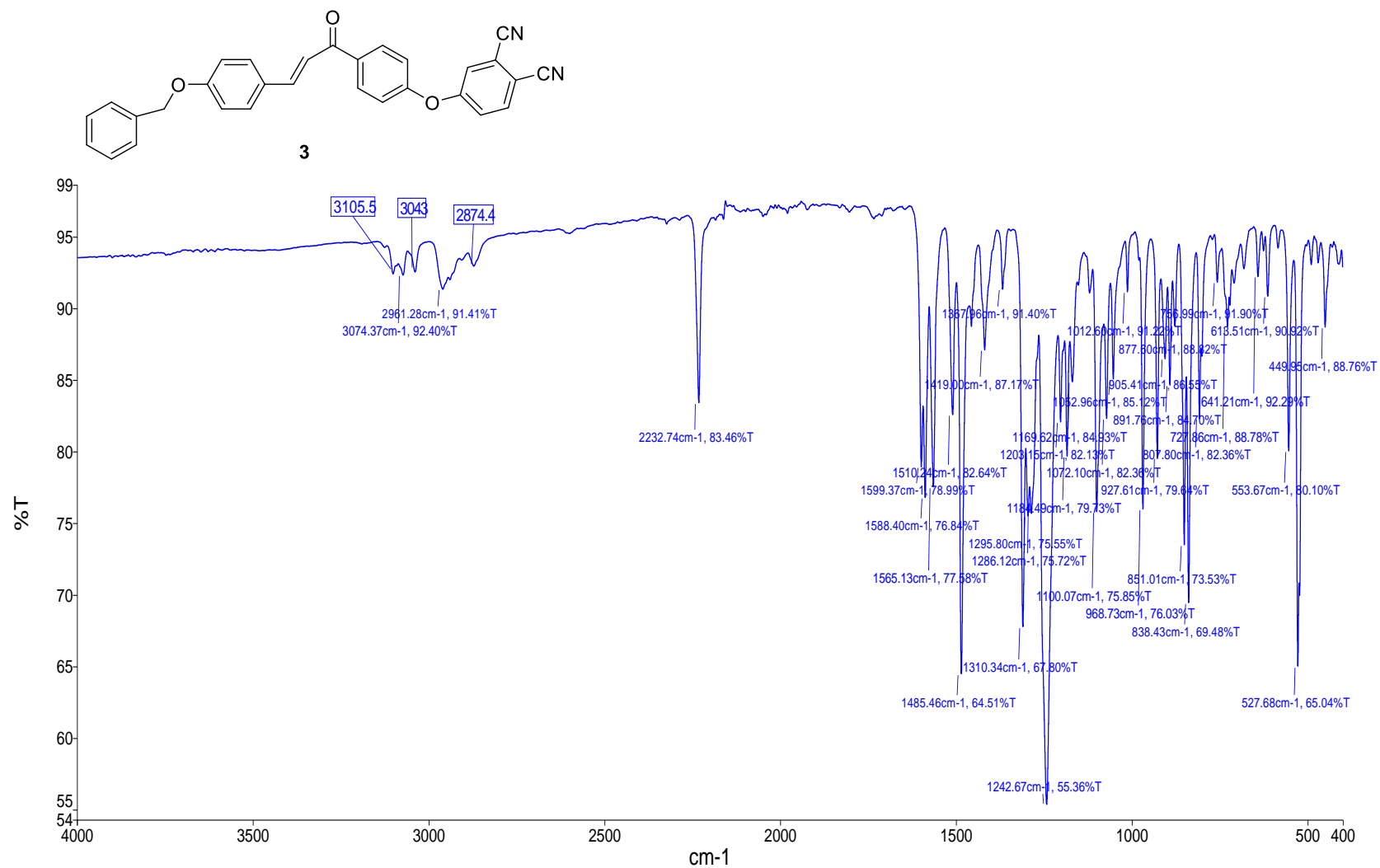


Figure S13: FT-IR spectrum of compound 3

© 2020 ACG Publications. All rights reserved.

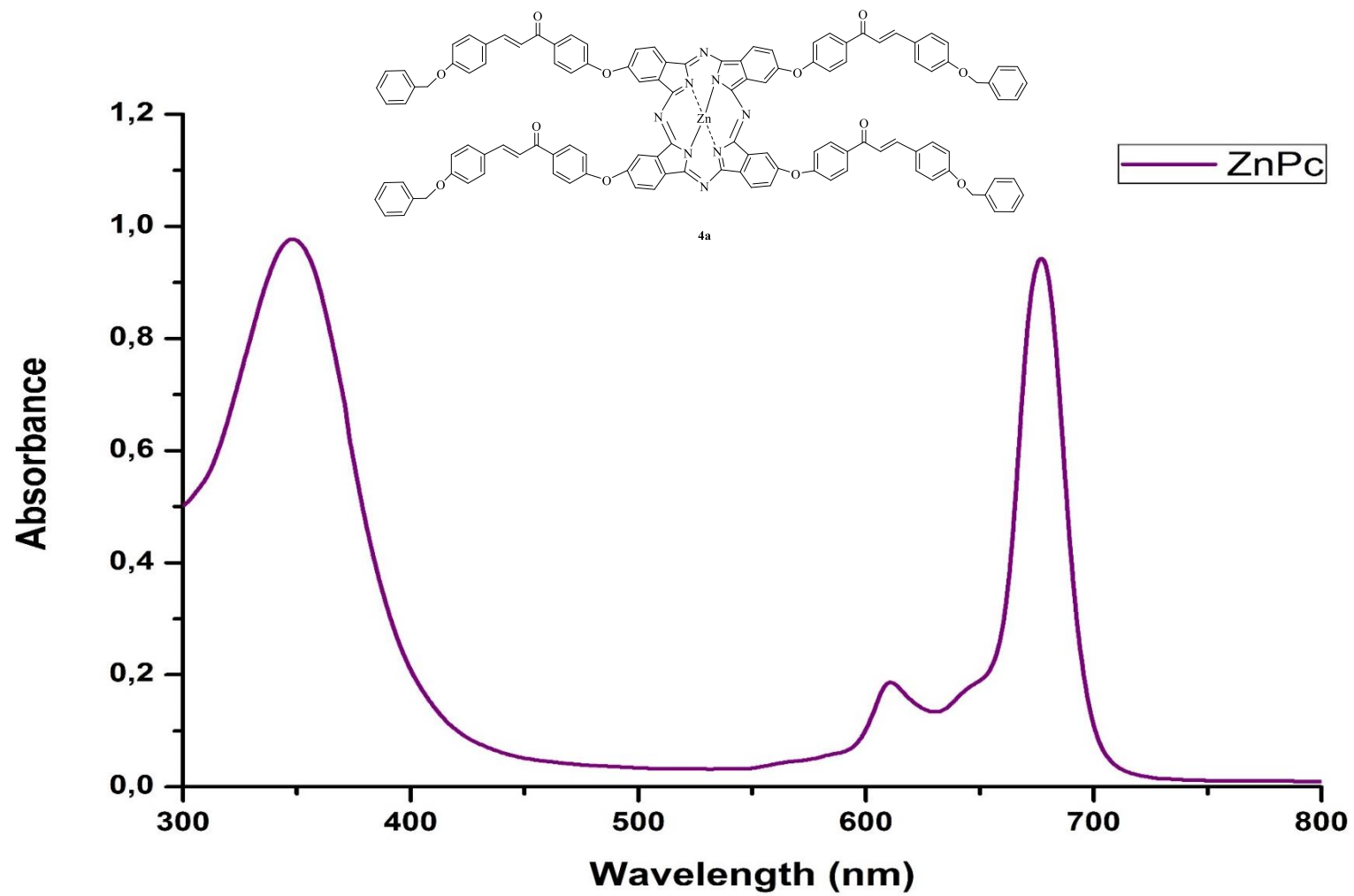
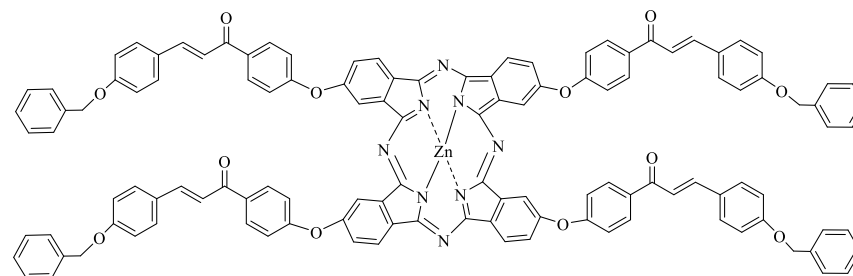


Figure S14: UV-Vis spectrum of compound **4a** (in DMF)

© 2020 ACG Publications. All rights reserved.



4a

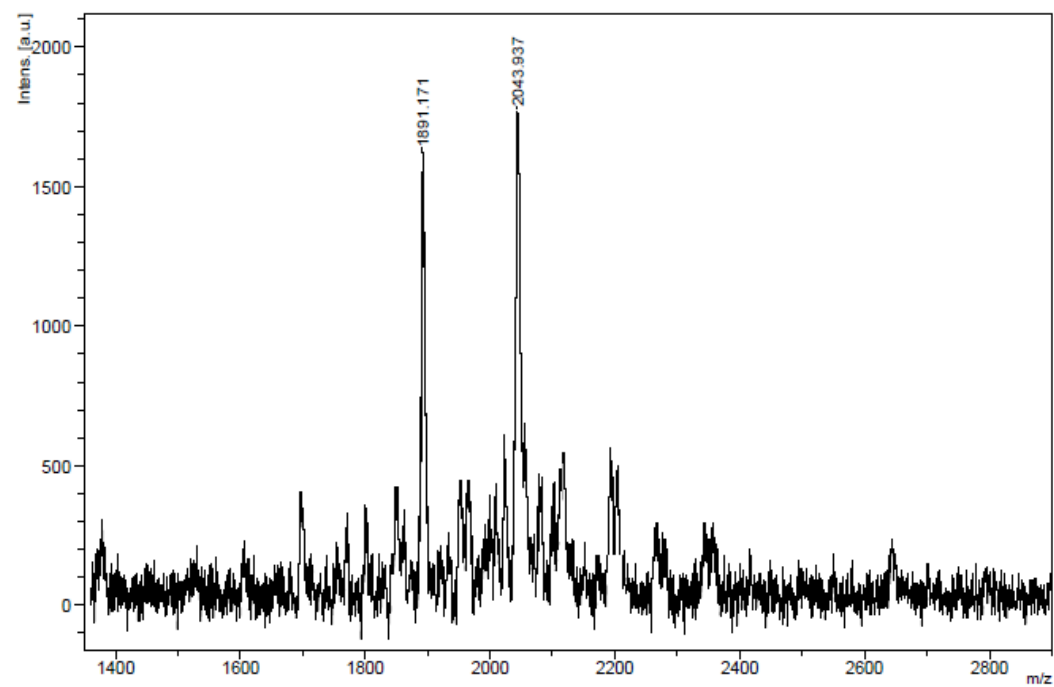


Figure S15: MALDI-TOF mass spectrum of compound **4a** in 1,8,9-anthracenetriol

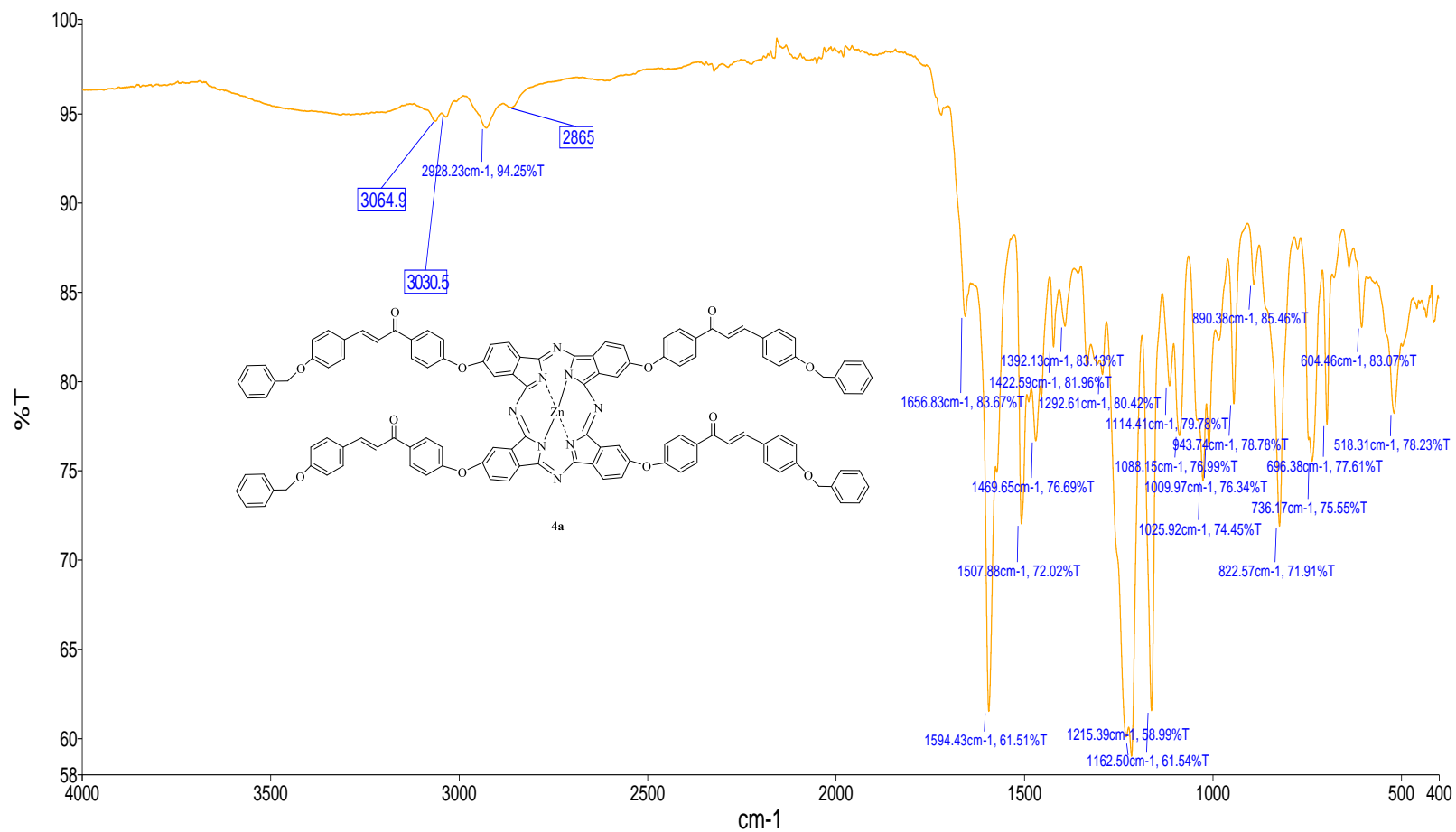


Figure S16: FT-IR spectrum of compound **4a**

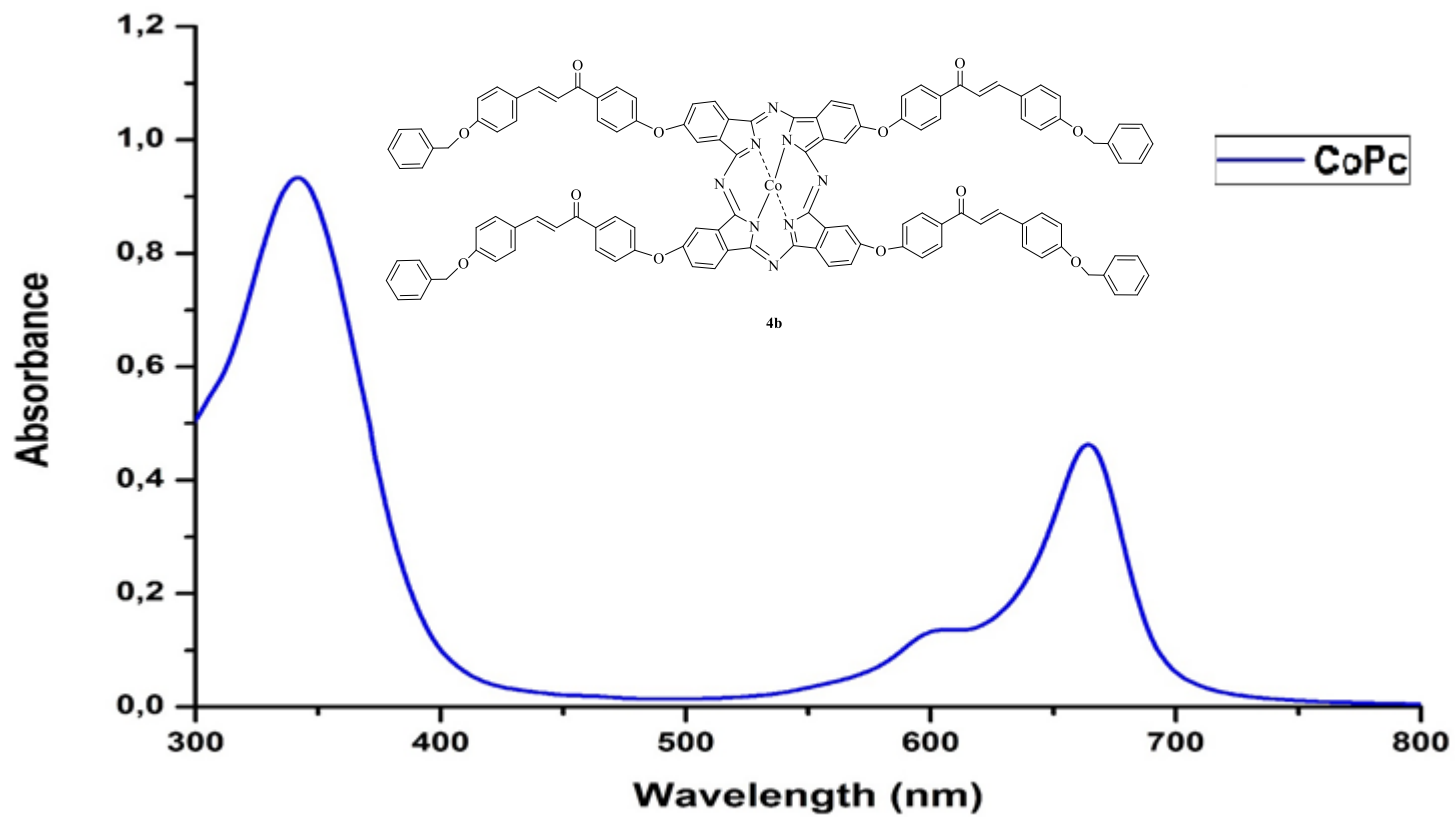


Figure S17: UV-Vis spectrum of compound **4b** (in DMF)

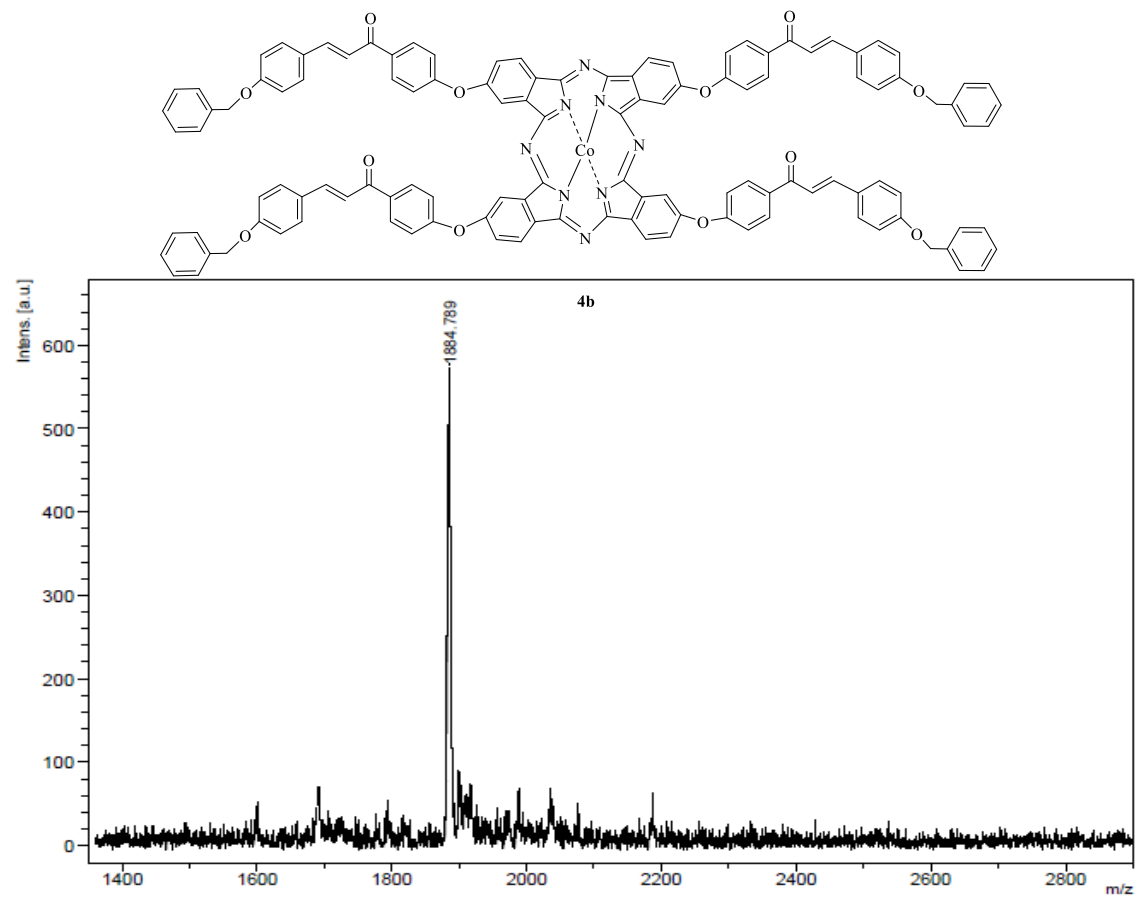


Figure S18: MALDI-TOF mass spectrum of **4b** in 1,8,9-anthracenetriol

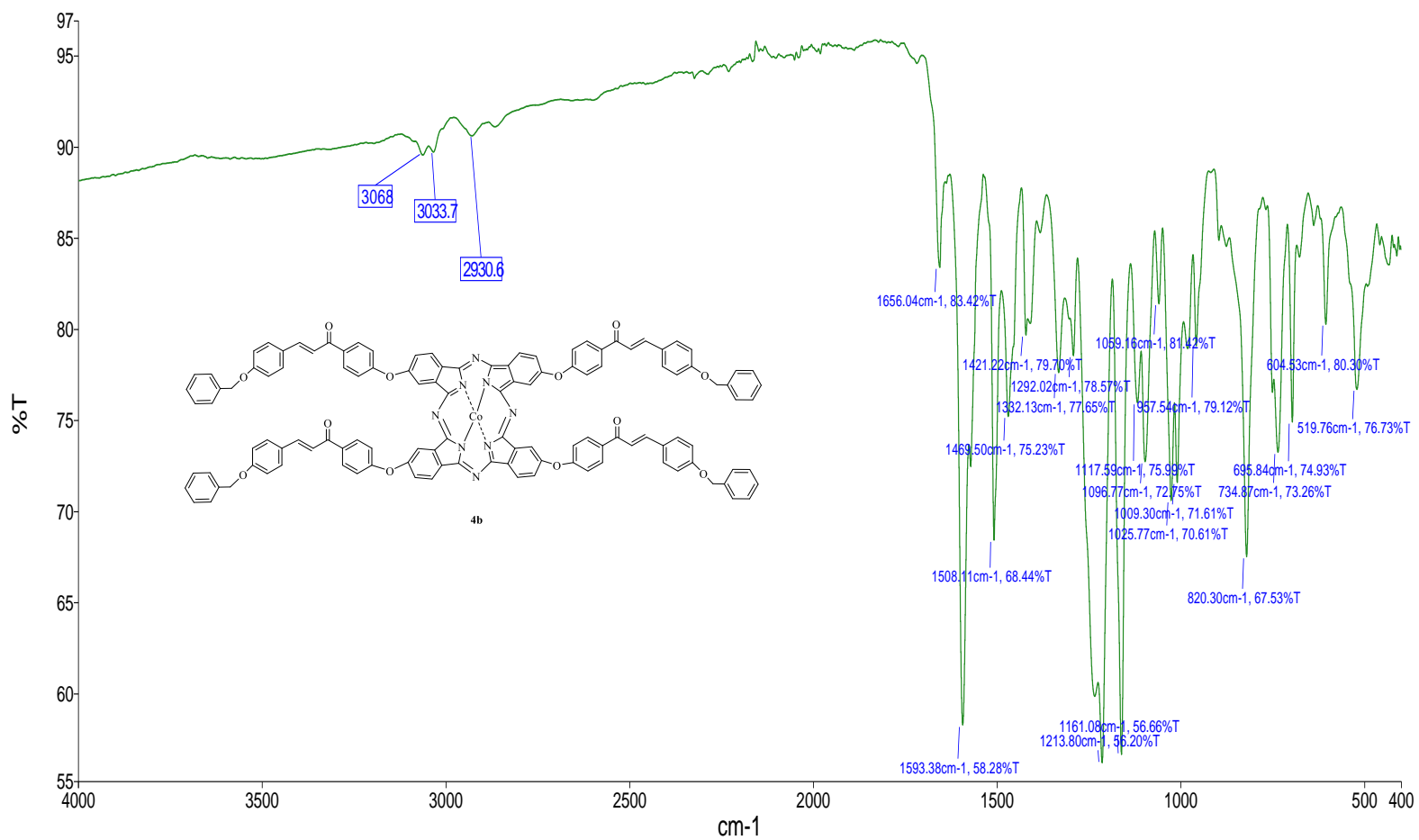
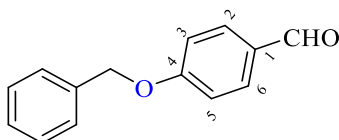


Figure S19: FT-IR spectrum of compound **4b**

© 2020 ACG Publications. All rights reserved.

S1: Structure Elucidation of Compounds 1-2

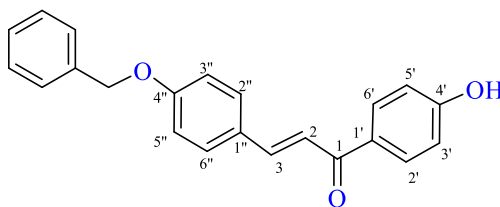
In the IR spectra of **1** (see Figure S3), Ar-H and aliphatic-H bands were observed at 3362 and 2829 cm^{-1} , respectively. In particular, the strong peak at 1685 cm^{-1} belongs to the aldehyde carbonyl group. The peaks at 1598 cm^{-1} , 1572 cm^{-1} and 1508 cm^{-1} were attributed to the carbon-carbon double bands of the aromatic ring. The most prominent peak at 1018 cm^{-1} is the C-O-C band.



benzyloxy)benzaldehyde (**1**)

^1H NMR spectra of compound **1** exhibited the CHO proton at 9.86 ppm as a singlet. While H_2/H_6 of the aromatic ring resonated as an AA' part of AA'BB' system giving quasi doublet at 7.82 ppm, H_3/H_5 resonated as BB' part of AA'BB' system giving doublet at 7.15 ppm. The resonance signal belongs to 5 H of phenyl appeared as multiplet between 7.48 – 7.32 ppm. The resonance signal of PhCH_2O gave a broad singlet at 5.12 ppm (Figure S1) Additionally, all ^{13}C -NMR signals are in agreement with structure (Figure S2).

IR spectra of compound **2** (Figure S6) exhibited hydroxyl stretching bands at 3059 and 3049 cm^{-1} . The aliphatic C-H strength was observed at 2849 cm^{-1} . While the C = O group of the aldehyde disappeared, the new peaks belong to the C=O and C = C bonds of the new compound appeared at 1641 cm^{-1} , 1597 cm^{-1} and 1586 cm^{-1} .



(*E*)-3-(4-(benzyloxy)phenyl)-1-(4-hydroxyphenyl)prop-2-en-1-one (**2**)

The resonance signal of H_2'/H_6' appeared as an AA' part of AA'BB' system as a quasi doublet at 7.97 ppm, and H_3'/H_5' gave BB' part of AA'BB' system as a quasi doublet at 7.10 ppm. Similarly, while $\text{H}_2''/\text{H}_6''$ arose as an AA' part of AA'BB' system as a quasi doublet at 7.62 ppm, $\text{H}_3''/\text{H}_5''$ were resonated as a quasi doublet as BB' part of AA'BB' system at 6.92 ppm. H_3 appeared as a doublet at 7.76 ppm ($J_{6,7} = 15.0$ Hz). 5 H of phenyl ring and H_2 resonated as a multiplet between 7.51-7.35 ppm and OCH_2 appeared as a singlet at 5.12 ppm (Figure S4). ^{13}C -NMR resonance frequencies of 16 carbons are fully compatible with the structure (Figure S5).